

Adaptive semiparametric Bayesian differential equations via sequential Monte Carlo

Shijia Wang

School of Statistics and Data Science, LPMC & KLMDASR, Nankai University, China
and

Liangliang Wang

Department of Statistics and Actuarial Science, Simon Fraser University, BC, Canada

May 1, 2022

Abstract

Nonlinear differential equations (DEs) are used in a wide range of scientific problems to model complex dynamic systems. The differential equations often contain unknown parameters that are of scientific interest, which have to be estimated from noisy measurements of the dynamic system. Generally, there is no closed-form solution for nonlinear DEs, and the likelihood surface for the parameter of interest is multi-modal and very sensitive to different parameter values. We propose a fully Bayesian framework for nonlinear DEs system. A flexible nonparametric function is used to represent the dynamic process such that expensive numerical solvers can be avoided. A sequential Monte Carlo in the annealing framework is proposed to conduct Bayesian inference for parameters in DEs. In our numerical experiments, we use examples of ordinary differential equations and delay differential equations to demonstrate the effectiveness of the proposed algorithm. We developed an R package that is available at <https://github.com/shijiaw/smcDE>.

Keywords: Differential Equations, sequential Monte Carlo, B-spline.

1 Introduction

Nonlinear differential equations (*e.g.* nonlinear ordinary or delay differential equations) are commonly used in modelling dynamic systems in ecology, physics and engineering. Delay differential equations (DDEs) are described by equations $d\mathbf{x}(t)/dt = \mathbf{g}(\mathbf{x}(t), \mathbf{x}(t - \tau)|\boldsymbol{\theta})$, where $\boldsymbol{\theta}$ is the vector of unknown parameters and τ is the time delay parameter. These are continuous time models for

interactions between variables $\mathbf{x}(t)$ and a time delay τ . Ordinary differential equations (ODEs) are often presented by $d\mathbf{x}(t)/dt = \mathbf{g}(\mathbf{x}(t)|\boldsymbol{\theta})$, which can be regarded as a special case of DDEs with $\tau = 0$. The form of $\mathbf{g}(\cdot)$ is generally proposed by specialists with scientific intuition. For example, ecologists proposed the simple Lotka-Volterra model (Rosenzweig and MacArthur, 1963) to understand and predict the population of predators and preys in ecosystems. Given a concrete form of the function $\mathbf{g}(\mathbf{x}(t), \mathbf{x}(t - \tau)|\boldsymbol{\theta})$, the parameters $\boldsymbol{\theta}$ and τ are unknown and required to be estimated using $\mathbf{y}(t)$ observed at some data points. We say that a DE is observed with measurement error. The observed $\mathbf{y}(t)$ is often assumed to link with variables $\mathbf{x}(t)$ through a linear regression such that $\mathbf{y}(t) = \mathbf{x}(t) + \boldsymbol{\epsilon}$, where $\boldsymbol{\epsilon}$ is measurement error. The estimation of parameters in DEs is of great interest and usually requires us to solve the DEs $d\mathbf{x}(t)/dt = \mathbf{g}(\mathbf{x}(t), \mathbf{x}(t - \tau)|\boldsymbol{\theta})$.

Most DE systems do not admit an analytic solution. One solution is to solve the DEs numerically (Butcher, 2016), for example by using the Euler method (Jain, 1979; Bulirsch and Stoer, 1966), the Exponential integrators (Hochbruck et al., 1998; Hochbruck and Ostermann, 2010) or the Runge-Kutta method (Jameson et al., 1981; Ascher et al., 1997). However, numerical DE solvers are computationally expensive, especially for DDEs. Various methods have been proposed to solve DEs more efficiently in recent decades. The idea of using smoothing splines to fit dynamic data was first proposed by Varah (1982). Ramsay and Silverman (2007), Poyton et al. (2006), Chen and Wu (2008) extended the idea of smoothing to a two-stage approach. In the first stage, spline coefficients are optimized by minimizing the sum of the squared distances between the data and the spline functions at the observation times. In the second stage, with the estimated spline coefficients, DE parameters are optimized by minimizing the residuals of DE models. The two-stage approach may lead to inconsistent estimates. Ramsay et al. (2007) proposed a generalized smoothing approach, called “parameter cascading”, based on data smoothing methods and a generalization of profiled estimation. In the proposed approach, the spline coefficients are treated as nuisance parameters. Their method iterates between optimizing the objective function with spline coefficients given parameter estimated so far, and optimizing the objective function with parameters given the estimated spline coefficients. The iteration is repeated until convergence is achieved. The parameter estimates are consistent and asymptotically normally distributed under mild conditions (Pang et al., 2017). There are several variants for the parameter cascading approach. Cao et al. (2011) proposed a robust algorithm to estimate measurements with outlier

based on smoothing splines. Cao et al. (2012) proposed a method to estimate time-varying parameter in ODEs, in which the ODE parameters are also modelled by smoothing splines. Wang and Cao (2012) defined a semiparametric method with smoothing spline to estimate DDE parameters.

Using smoothing splines to model DEs are computationally efficient since we do not require to numerically solve DEs. Most methods based on data smoothing to estimate parameters of DEs are derived from a frequentist perspective, which means they are only able to provide point estimates for the DE parameters. Bayesian methods are of interest since they provide the uncertainty of parameters. Campbell and Steele (2012) proposed a smooth functional tempering algorithm to conduct posterior inference for ODEs parameters. This idea originates from parallel tempering and model based smoothing. Zhang et al. (2017) proposed a high dimensional linear ordinary differential equation (ODE) model to accommodate the directional interaction in brain areas. Parallelized schemes for Markov chain Monte Carlo have been proposed to estimate the model. Bhaumik et al. (2015) investigated a two-stage procedure to estimate the parameter by minimizing the penalized ODEs.

There are several lines of work involved in estimating DEs parameter from a Bayesian perspective based on numerical DE solver. Dass et al. (2017) proposed a two-step approach to approximate posterior distributions for parameters of interest. They first applied a numerical algorithm to solve ODEs, then integrated nuisance parameters using Laplace approximations. Bhaumik et al. (2017) proposed a modification of Bhaumik et al. (2015) by directly considering the distance between the function in the nonparametric model and that obtained from a four stage Runge-Kutta (RK4) method. Calderhead et al. (2009) presented a novel Bayesian sampler to infer parameters in non-linear delay differential equations, the derivatives and time delay parameters were estimated via Gaussian processes. To make the DE estimation more consistent, Dondelinger et al. (2013) proposed an adaptive gradient matching approach to jointly infer the hyperparameters of a Gaussian process as well as ODE parameters. Barber and Wang (2014) simplified previous approaches by proposing a more natural generative model of data using Gaussian process, which directly links state derivative information with system observations.

Standard sequential Monte Carlo (SMC) methods (Doucet et al., 2001, 2000; Liu and Chen, 1998) are popular approaches for estimating dynamic models (e.g. state space models). SMC methods combine importance sampling and resampling algorithms. Under mild conditions, con-

sistency properties and asymptotic normality hold (Chopin et al., 2004). Del Moral et al. (2006) proposed a general SMC framework, to sample sequentially from a sequence of intermediate probability distributions that are defined on a common space. Several SMC methods have been proposed to estimate parameters in ODE models. Zhou et al. (2016) presented an adaptive sequential Monte Carlo sampling strategy to estimate parameters and conduct model selection. They used an example of ODEs to demonstrate the performance of model selection using their proposed algorithm. Lee et al. (2018) introduced additive Gaussian errors into numerically solved ODE trajectory, and they proposed a particle filter to infer ODE parameters. In addition, Gaussian process has been used to avoid numerical integration. These works are based on numerically solving ODE models.

In this article, we propose to use an efficient annealed SMC to conduct Bayesian inference for parameters in nonlinear DEs. The proposed method is a Bayesian semi-parametric approach in which DE trajectories are represented using a linear combination of basis functions. Consequently, our method avoids expensive numerical solvers, especially those for DDEs. It instead needs to estimate the basis coefficients together with other parameters in the DEs. In other words, the parameters of interest include the DE parameters and basis coefficients of smoothing spline functions. In addition, the tuning parameter is estimated using a fully Bayesian approach, which avoids tuning through expensive cross-validation. We propose an annealed sequential Monte Carlo algorithm to effectively sample parameters with multiple isolated posterior modes and basis function coefficients of high dimensionality. The proposed annealed SMC adopts the adaptive scheme in Zhou et al. (2016) to choose the sequence of the tempering parameters that determine the intermediate target distributions of the SMC. Our numerical experiments demonstrate the effectiveness of our algorithm in estimating parameters and DE trajectories for both ODEs and DDEs cases.

The rest of article is organized as follows. In *Section 2*, we construct a fully Bayesian framework for nonlinear DEs. In *Section 3*, we introduce our new algorithm for Bayesian inference for nonlinear DEs. In *Section 4* and *Section 5*, we use numerical experiments to show the effectiveness of our method. We conclude in *Section 6*.

2 Hierarchical Bayesian differential equations

In this section, we introduce a hierarchical Bayesian structure for DE models. In *Section 2.1*, we introduce the likelihood function for DEs. In *Section 2.2*, we construct a fully Bayesian model for

the DE model. In *Section 2.3*, we introduce selection of the tuning parameter λ .

2.1 DE models

We use $\mathbf{x}(t) = (x_1(t), \dots, x_I(t))'$ to denote the DE variables, where $x_i(t)$ denotes the i -th DE variable, and I denotes the total number of DE variables. Each DE variable $x_i(t), i = 1, \dots, I$, is a dynamic process modelled with one differential equation

$$\begin{aligned} \frac{dx_i(t)}{dt} &= g_i(\mathbf{x}(t), \mathbf{x}(t - \tau) | \boldsymbol{\theta}), \\ x_i(0) &= x_{i0}, \end{aligned} \tag{1}$$

where $\boldsymbol{\theta}$ denotes the vector of unknown parameters in the DE model, τ is the delay parameter in DDE model ($\tau = 0$ in ODE model), and $x_i(0)$ is the initial condition for the i -th DE variable, which is also unknown and needs to be estimated. Delay differential equations (DDEs) are time-delayed systems, with a delay parameter τ . The time delay in DDEs considers the dependence of the present state of the DE variable based on its past state. In DDEs, $x_i(t - \tau) = x_{i0}$ for $t < \tau$. We refer readers to *Section 4* for a more detailed description of DDE models.

We do not observe the DEs directly, instead we observe them with measurement error. We let $\mathbf{y}_i = (y_{i1}, \dots, y_{iJ})'$ denote the observations for the i -th DE trajectory. The j -th observation of \mathbf{y}_i is assumed to be normally distributed with mean $x_i(t_{ij} | \boldsymbol{\theta}, \tau, x_{i0})$ and variance σ_i^2 ,

$$y_{ij} \sim N(x_i(t_{ij} | \boldsymbol{\theta}, \tau, x_{i0}), \sigma_i^2), j = 1, \dots, J,$$

where $x_i(t_{ij} | \boldsymbol{\theta}, \tau, x_{i0})$ denotes the DE solution given $\boldsymbol{\theta}$, τ and initial condition x_{i0} .

The joint likelihood function of $\boldsymbol{\theta}$, τ , $\mathbf{x}(0)$ and σ_i^2 admits the following form

$$L(\boldsymbol{\theta}, \tau, \mathbf{x}(0), \sigma_i^2) = \prod_{i=1}^I \prod_{j=1}^J (\sigma_i^2)^{-1/2} \exp \left\{ - \frac{(y_{ij} - x_i(t_{ij} | \boldsymbol{\theta}, \tau, \mathbf{x}(0)))^2}{2\sigma_i^2} \right\}. \tag{2}$$

We use a figure (see Figure 1 (b)) to show an example of the log-likelihood surface over DEs parameters $\boldsymbol{\theta}$, and for the setup of this model we refer to *Section 5.1*. The log-likelihood surface for $\boldsymbol{\theta}$ has multiple isolated modes, and it is very sensitive to different parameter values.

2.2 A fully Bayesian structure for DE model

Numerically solving DEs can be computationally extremely intensive, especially for DDE models. We propose to solve differential equations by penalized smoothing. More specifically, we repre-

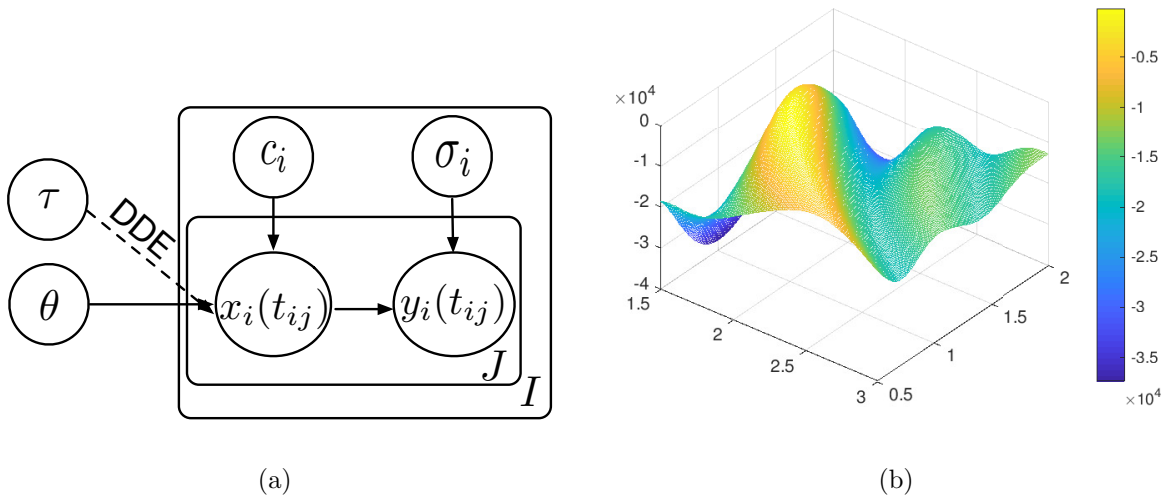


Figure 1: (a) Graphical representation of DEs, (b) Log-likelihood surface for a DE model.

sent the i -th DE function $x_i(t)$ as a linear combination of L_i B-spline basis functions $\Phi(t) = (\phi_1(t), \phi_2(t), \dots, \phi_{L_i}(t))'$ (see Figure 2 for an example of cubic B-spline functions (Ramsay, 2004; De Boor, 1972)),

$$x_i(t) = \Phi(t)' \mathbf{c}_i,$$

where \mathbf{c}_i denotes the vector of basis coefficients. The initial condition for the i -th DE function is $x_i(0) = \Phi(0)' \mathbf{c}_i$. One advantage of using smoothing spline functions to model DE trajectories is that we can avoid estimating the initial condition $\mathbf{x}(0)$; instead, it is estimated using $\hat{x}_i(t) = \Phi(t)' \hat{\mathbf{c}}_i$, where $\hat{\mathbf{c}}_i$ is the vector of estimated basis coefficients. Figure 1 (a) represents the graphical structure for the proposed DE model. The unknown parameters in our DE model include spline coefficients \mathbf{c}_i , the delay time parameter τ (which is known in ODE with $\tau = 0$), the DE parameter θ , and variance parameter σ_i^2 .

In Bayesian smoothing approaches, we give $\mathbf{x}(t)$ a prior density proportional to the “partially improper” Gaussian process (Berry et al., 2002). We let λ denote the smoothing parameter for the penalty term. This smoothing parameter λ controls the trade-off between fit to the data and

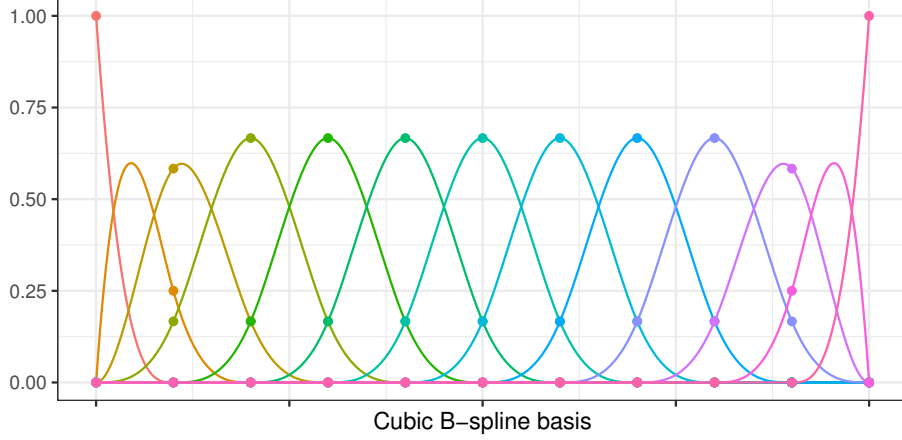


Figure 2: The thirteen B-spline basis functions defined on $[0, 1]$ with degree three and nine equally spaced knots.

fidelity to the DE model. Given λ , the prior distribution for $\mathbf{x}(t)$ is

$$\begin{aligned} p(\mathbf{x}(t)|\boldsymbol{\theta}, \mathbf{c}, \tau) &\propto \exp \left\{ -\frac{\lambda}{2} \sum_{i=1}^I \int_{t_1}^{t_J} \left[\frac{dx_i(s)}{ds} - g(\mathbf{x}(s), \mathbf{x}(s - \tau)|\boldsymbol{\theta}) \right]^2 ds \right\}, \\ &= \exp \left\{ -\frac{\lambda}{2} \sum_{i=1}^I \int_{t_1}^{t_J} \left[\frac{d\boldsymbol{\Phi}(s)'}{ds} \mathbf{c}_i - g_i(\boldsymbol{\Phi}(s)' \mathbf{c}, \boldsymbol{\Phi}(s - \tau)' \mathbf{c} | \boldsymbol{\theta}) \right]^2 ds \right\}, \end{aligned}$$

where $\boldsymbol{\Phi}(s - \tau) = \boldsymbol{\Phi}(0)$ if $s < \tau$. This prior distribution measures how well the estimated DE variables $\hat{\mathbf{x}}(t)$ satisfy the DE system. Details on selecting a proper λ will be discussed in *Section 2.3*.

In the fully Bayesian framework, we need to assign appropriate priors for model parameters $\boldsymbol{\theta}$, τ , \mathbf{c}_i , σ_i^2 , $i = 1, \dots, I$. The following priors are specified:

$$\boldsymbol{\theta} \sim MVN(\mathbf{0}_D, \sigma_\theta^2 \mathbf{I}_D), \quad (3)$$

$$\tau \sim U(t_1, t_J), \quad (4)$$

$$\mathbf{c}_i \sim MVN(\mathbf{0}_L, \sigma_c^2 \mathbf{I}_{L_i}), \quad i = 1, \dots, I, \quad (5)$$

$$\sigma_i^2 \sim IG(g_0, h_0), \quad i = 1, \dots, I, \quad (6)$$

where σ_θ^2 , σ_c^2 , g_0 and h_0 are the hyper-parameters in prior distributions, and D is the dimension of the vector $\boldsymbol{\theta}$. The vector of all zeros is represented by $\mathbf{0}$, and \mathbf{I} is an identity matrix. Their subscripts denote the vector/matrix dimension.

We introduce a new notation $\boldsymbol{\beta} = (\tau, \boldsymbol{\theta}, \mathbf{c}, \boldsymbol{\sigma})'$ to denote all the parameters of interest. Let $p(\mathbf{y}|\boldsymbol{\beta})$ denote the penalized likelihood function as follows

$$p(\mathbf{y}|\boldsymbol{\beta}) \propto \left(\prod_{i=1}^I \prod_{j=1}^J \sigma_i^2 \right)^{-1/2} \exp \left\{ - \sum_{i=1}^I \left(\sum_{j=1}^J \frac{(y_{ij} - \boldsymbol{\Phi}(t_{ij})' \mathbf{c}_i)^2}{2\sigma_i^2} + \frac{\lambda}{2} \int_{t_1}^{t_J} \left[\frac{d\boldsymbol{\Phi}(s)'}{ds} \mathbf{c}_i - g_i(\boldsymbol{\Phi}(s)' \mathbf{c}, \boldsymbol{\Phi}(s - \tau)' \mathbf{c} | \boldsymbol{\theta}) \right]^2 ds \right) \right\}.$$

The integral

$$\mathbf{R}_{ij} = \int_{t_j}^{t_{j+1}} \left[\frac{d\boldsymbol{\Phi}(s)'}{ds} \mathbf{c}_i - g_i(\boldsymbol{\Phi}(s)' \mathbf{c}, \boldsymbol{\Phi}(s - \tau)' \mathbf{c} | \boldsymbol{\theta}) \right]^2 ds.$$

usually does not have a closed-form expression. However, it can be evaluated by numerical quadrature approximation. We approximate the integral by using the composite Simpson's rule (Burden et al., 2001)

$$\mathbf{R}_{ij} = \sum_{m=1}^M v_{jm} \cdot \left(\left[\frac{d\boldsymbol{\Phi}(s)'}{ds} \mathbf{c}_i - g_i(\boldsymbol{\Phi}(s)' \mathbf{c}, \boldsymbol{\Phi}(s - \tau)' \mathbf{c} | \boldsymbol{\theta}) \right]^2 \Big|_{s=t_{jm}} \right),$$

where M is the number of quadrature points, t_{jm} is the m -th quadrature point in $[t_j, t_{j+1}]$, and v_{jm} is the corresponding quadrature weight.

Let $\pi_0(\boldsymbol{\beta})$ denote the prior distribution, which is specified in Equations (3) to (6). We are interested in the normalized posterior distribution for $\boldsymbol{\beta}$

$$\pi(\boldsymbol{\beta}) = \frac{\gamma(\boldsymbol{\beta})}{Z} = \frac{\pi_0(\boldsymbol{\beta})p(\mathbf{y}|\boldsymbol{\beta})}{Z},$$

where $\gamma(\boldsymbol{\beta}) = \pi_0(\boldsymbol{\beta})p(\mathbf{y}|\boldsymbol{\beta})$ is the unnormalized posterior distribution of $\boldsymbol{\beta}$, and $Z = \int \pi_0(\boldsymbol{\beta})p(\mathbf{y}|\boldsymbol{\beta})d\boldsymbol{\beta}$ is the marginal likelihood. The unnormalized posterior distribution of $\boldsymbol{\beta}$ can be written as

$$\begin{aligned} \gamma(\boldsymbol{\beta}) = & \left(\prod_{i=1}^I \prod_{j=1}^J \sigma_i^2 \right)^{-1/2} \exp \left\{ - \sum_{i=1}^I \left(\sum_{j=1}^J \frac{(y_{ij} - \boldsymbol{\Phi}(t_{ij})' \mathbf{c}_i)^2}{2\sigma_i^2} + \frac{\lambda}{2} \int_{t_1}^{t_J} \left[\frac{d\boldsymbol{\Phi}(s)'}{ds} \mathbf{c}_i - g_i(\boldsymbol{\Phi}(s)' \mathbf{c}, \boldsymbol{\Phi}(s - \tau)' \mathbf{c} | \boldsymbol{\theta}) \right]^2 ds \right) \right\} \\ & \cdot \left(\prod_{i=1}^I \sigma_i^2 \right)^{-g_0-1} \exp \left\{ - \sum_{i=1}^I \frac{h_0}{\sigma_i^2} \right\} \cdot \exp \left\{ - \sum_{i=1}^I \frac{\mathbf{c}'_i \mathbf{c}_i}{\sigma_c^2} \right\} \exp \left\{ - \frac{\boldsymbol{\theta}' \boldsymbol{\theta}}{\sigma_\theta^2} \right\}. \end{aligned}$$

The marginal likelihood $Z = \int \gamma(\boldsymbol{\beta})d\boldsymbol{\beta}$ is intractable.

2.3 The choice of λ

The tuning parameter λ is important in balancing between fit to the data and fidelity to the DE model. A small value of λ does not impose much information about the DE fitting. If $\lambda \rightarrow 0$,

we end up fitting least squares for spline coefficients with the data. If we choose a large value of λ , the prior information of DE system is too strong and not much information about the data is taken into consideration. Hence, it is crucial to choose a proper value of λ to balance the DE fitting and data information.

One approach to choose λ is through cross-validation (Wang and Cao, 2012; Reiss and Todd Ogdén, 2009) from a range of reasonable choices of λ . However, this approach is infeasible in Bayesian frameworks as it significantly increases the computational cost. We propose to treat λ as an unknown parameter by specifying a prior distribution on λ and estimating its posterior distribution through a fully Bayesian method. This idea is adapted from Berry et al. (2002), in which they automatically select a smoothing parameter for splines. We choose the prior distribution for the smoothing parameter to be $Gamma(a_\lambda, b_\lambda)$.

3 Methodology

One classical methodology for Bayesian inference of nonlinear DE parameters is Markov chain Monte Carlo (MCMC). In MCMC, we construct an ergodic Markov chain which admits the normalized posterior as its stationary distribution. If we run the chain long enough, convergence to the posterior is guaranteed. We show the details of this method in the Appendix.

However, Markov chain Monte Carlo (more specifically, the Metropolis Hastings (MH) algorithm) is inefficient for estimating parameters of nonlinear DEs for several reasons. First, the posterior surface is extremely sensitive to DE parameters θ . There may exist isolated modes in the posterior distribution. The posterior may change quite a bit even with a tiny change in parameter value. Second, the computation of likelihood function involves numerically solving nonlinear DEs, which is computationally expensive. Third, the convergence of MCMC is generally difficult to assess.

In *Section 3.1*, we propose an SMC method for nonlinear DE inference based on the Bayesian hierarchical structure proposed in *Section 2*. In *Section 3.2*, we discuss some properties of our SMC method. In *Section 3.3*, we introduce an advanced scheme to adaptively determine the intermediate target distributions in SMC.

3.1 An annealed sequential Monte Carlo for Bayesian DE inference

As described in *Section 2.3* that λ is treated as an unknown parameter of the model, we define $\boldsymbol{\beta} = (\tau, \boldsymbol{\theta}, \mathbf{c}, \boldsymbol{\sigma}, \lambda)'$. To better cope with the inadequates of MCMC, we propose a sequential Monte Carlo (SMC) algorithm in the SMC (Del Moral et al., 2006) framework for the *static* setting for Bayesian DEs. This special case of SMC is a generic method to approximate a sequence of intermediate probability distributions $\{\pi_r(\boldsymbol{\beta})\}_{0 \leq r \leq R}$ defined on a common measurable space (E, \mathcal{E}) . This method is different from the standard SMC algorithm (Doucet et al., 2000, 2001), as the sequence of intermediate probability distributions $\{\pi_r(\boldsymbol{\beta})\}_{0 \leq r \leq R}$ in standard SMC methods are generally defined on measurable spaces with incremental dimension.

The SMC algorithm in the static setting approximates the target distribution $\pi(\boldsymbol{\beta})$ in R steps. At each step r , we use a list of K samples to represent $\pi_r(\boldsymbol{\beta})$, denoted by $\{\boldsymbol{\beta}_{k,r}\}_{k=1,2,\dots,K}$. Each of these K samples is called a particle. There is a positive weight associated with each particle $\boldsymbol{\beta}_{k,r}$. We use $w_{k,r}$ to denote the unnormalized weight of $\boldsymbol{\beta}_{k,r}$ and use $W_{k,r}$ to be the corresponding normalized weight. From iteration r to $r+1$, we move particles from $\{\boldsymbol{\beta}_{k,r}\}_{k=1,2,\dots,K}$ to $\{\boldsymbol{\beta}_{k,r+1}\}_{k=1,2,\dots,K}$ by using a Markov kernel, denoted by $T_{r+1}(\boldsymbol{\beta}_{k,r}, \boldsymbol{\beta}_{k,r+1})$. Then we compensate the difference between the particles $\boldsymbol{\beta}_{k,r+1}$ proposed from $\{T_{r+1}(\boldsymbol{\beta}_{k,r}, \boldsymbol{\beta}_{k,r+1})\}_{k=1,\dots,K}$ and $\pi_r(\boldsymbol{\beta})$ by the updated weights $W_{k,r+1}$. To get $W_{k,r+1}$, we first compute the incremental importance weight

$$\tilde{w}_{k,r+1} = \frac{\gamma_{r+1}(\boldsymbol{\beta}_{k,r+1})L_r(\boldsymbol{\beta}_{k,r+1}, \boldsymbol{\beta}_{k,r})}{\gamma_r(\boldsymbol{\beta}_{k,r})T_{r+1}(\boldsymbol{\beta}_{k,r}, \boldsymbol{\beta}_{k,r+1})},$$

where $L_r(\boldsymbol{\beta}_{k,r+1}, \boldsymbol{\beta}_{k,r})$ is the artificial backward kernel (Del Moral et al., 2006, 2012), denoting the probability of moving from $\boldsymbol{\beta}_{k,r+1}$ to $\boldsymbol{\beta}_{k,r}$. Then we calculate the unnormalized weight by using the previous unnormalized weight and the incremental importance weight as follows

$$w_{k,r+1} = w_{k,r} \cdot \tilde{w}_{k,r+1}.$$

The normalized weights $W_{k,r+1}$ are obtained by $W_{k,r+1} = w_{k,r+1} / (\sum_{k=1}^K w_{k,r+1})$.

The selection of the backward kernel $L_r(\boldsymbol{\beta}_{k,r+1}, \boldsymbol{\beta}_{k,r})$ is important as it will impact the variance of $\{W_{k,r+1}\}_{k=1,\dots,K}$. We refer readers to Del Moral et al. (2006) for a more detailed discussion of this artificial backward kernel. One typical approach in the SMC framework for the static setting is to select $T_{r+1}(\boldsymbol{\beta}_{k,r}, \boldsymbol{\beta}_{k,r+1})$ to be a π_{r+1} -invariant MCMC kernel. A convenient backward Markov

kernel that allows an easy evaluation of the importance weight is

$$L_r(\boldsymbol{\beta}_{k,r+1}, \boldsymbol{\beta}_{k,r}) = \frac{\pi_{r+1}(\boldsymbol{\beta}_{k,r})T_{r+1}(\boldsymbol{\beta}_{k,r}, \boldsymbol{\beta}_{k,r+1})}{\pi_{r+1}(\boldsymbol{\beta}_{k,r+1})}.$$

With this backward kernel, the weight update function $\tilde{w}_{k,r+1}$ becomes

$$\begin{aligned} \tilde{w}_{k,r+1} &= \frac{\gamma_{r+1}(\boldsymbol{\beta}_{k,r+1})L_r(\boldsymbol{\beta}_{k,r+1}, \boldsymbol{\beta}_{k,r})}{\gamma_r(\boldsymbol{\beta}_{k,r})T_{r+1}(\boldsymbol{\beta}_{k,r}, \boldsymbol{\beta}_{k,r+1})} \\ &= \frac{\gamma_{r+1}(\boldsymbol{\beta}_{k,r+1})}{\gamma_r(\boldsymbol{\beta}_{k,r})} \cdot \frac{\pi_{r+1}(\boldsymbol{\beta}_{k,r})T_{r+1}(\boldsymbol{\beta}_{k,r}, \boldsymbol{\beta}_{k,r+1})}{\pi_{r+1}(\boldsymbol{\beta}_{k,r+1})} \cdot \frac{1}{T_{r+1}(\boldsymbol{\beta}_{k,r}, \boldsymbol{\beta}_{k,r+1})} \\ &= \frac{\gamma_{r+1}(\boldsymbol{\beta}_{k,r})}{\gamma_r(\boldsymbol{\beta}_{k,r})}. \end{aligned}$$

Thus, we do not require pointwise evaluation of the forward kernel $T_{r+1}(\boldsymbol{\beta}_{k,r}, \boldsymbol{\beta}_{k,r+1})$ and the backward kernel $L_r(\boldsymbol{\beta}_{k,r+1}, \boldsymbol{\beta}_{k,r})$ to compute the weight function.

In this article, we propose a sequence of annealing intermediate target distributions (Neal, 2001; Wang et al., 2019) $\{\pi_r(\boldsymbol{\beta})\}_{0 \leq r \leq R}$ to facilitate the exploration of posterior space, such that

$$\pi_r(\boldsymbol{\beta}) \propto \gamma_r(\boldsymbol{\beta}) = p(\mathbf{y}|\boldsymbol{\beta})^{\alpha_r} \pi_0(\boldsymbol{\beta}),$$

where $0 = \alpha_0 < \alpha_1 < \dots < \alpha_{R-1} < \alpha_R = 1$ is the sequence of annealing parameters. If there are isolated modes in $\pi(\boldsymbol{\beta})$, MCMC may get stuck in one of the modes which is close to the initial value. Introducing a series of powered posterior distribution is to avoid this. With a small annealing parameter α_r , the intermediate posterior surface is flat, which makes samples easier to move across modes. The intermediate posterior target with a higher value of annealing parameter is closer to the true posterior. The samples move closer to the target posterior distribution if we increase α_r . One simple choice of annealing parameters is to equally put parameters across $[0, 1]$, such that $\alpha_0 = 0, \alpha_1 = 1/R, \alpha_2 = 2/R, \dots, \alpha_{R-1} = (R-1)/R, \alpha_R = 1$.

We now introduce an SMC algorithm with a defined sequence of intermediate targets. First, we initialize particles $\{\boldsymbol{\beta}_{k,0}\}_{k=1,2,\dots,K}$. At each step $r-1$, we keep a list of K particles $\{\boldsymbol{\beta}_{k,r-1}\}_{k=1,2,\dots,K}$ in memory. We let $\{\tilde{\boldsymbol{\beta}}_{k,r-1}\}_{k=1,2,\dots,K}$ denote particles after resampling step (see *Step 3*). We iterate between the following three steps to obtain the approximated intermediate target posterior

$$\hat{\pi}_r(\boldsymbol{\beta}) = \sum_{k=1}^K W_{k,r} \cdot \delta_{\boldsymbol{\beta}_{k,r}}(\boldsymbol{\beta}), \quad (r = 1, \dots, R).$$

Step 1. We compute the weight function for particles at iteration r with

$$W_{k,r} \propto w_{k,r} = w_{k,r-1} \cdot \frac{\gamma_r(\tilde{\boldsymbol{\beta}}_{k,r-1})}{\gamma_{r-1}(\tilde{\boldsymbol{\beta}}_{k,r-1})} = w_{k,r-1} \cdot p(\mathbf{y}|\tilde{\boldsymbol{\beta}}_{k,r-1})^{\alpha_r - \alpha_{r-1}}. \quad (7)$$

Note that the weight update function for particles at the r -th iteration only depends on particles at the $(r - 1)$ -th iteration, which is different from the standard SMC algorithm (Doucet et al., 2000, 2001).

Step 2. We propagate new samples $\{\boldsymbol{\beta}_{k,r}\}_{k=1,\dots,K}$ via π_r -invariant MCMC moves, $\{\boldsymbol{\beta}_{k,r} \sim T_r(\tilde{\boldsymbol{\beta}}_{k,r-1}, \cdot)\}_{k=1,\dots,K}$. The conditional posterior distributions, $\pi_r(\sigma_i^2|\mathbf{c}_i)$, $\pi_r(\tau|\mathbf{c}, \boldsymbol{\theta}, \lambda)$, $\pi_r(\boldsymbol{\theta}|\mathbf{c}, \tau, \lambda)$ and $\pi_r(\mathbf{c}_i|\tau, \boldsymbol{\theta}, \boldsymbol{\sigma}, \mathbf{c}_{-i}, \lambda)$ admit the following forms

- The full conditional distribution for σ_i^2 admits π_r -invariant is

$$\sigma_i^2|\mathbf{c}_i \sim IG\left(g_0 + \frac{J}{2}, h_0 + \frac{\alpha_r}{2} \sum_{j=1}^J (y_{ij} - \boldsymbol{\Phi}(t_{ij})'\mathbf{c}_i)^2\right). \quad (8)$$

- The conditional distribution $\pi_r(\tau|\mathbf{c}, \boldsymbol{\theta}, \lambda)$ does not admit a closed form.

$$\begin{aligned} \gamma_r(\tau|\mathbf{c}, \boldsymbol{\theta}, \lambda) &\propto \\ \exp\left\{-\alpha_r \sum_{i=1}^I \sum_{j=1}^J \left(\frac{\lambda}{2} \sum_{m=1}^M v_{jm} \cdot \left(\left[\frac{d\boldsymbol{\Phi}(s)'}{ds} \mathbf{c}_i - g_i(\boldsymbol{\Phi}(s)'\mathbf{c}|\boldsymbol{\theta}) - \boldsymbol{\Phi}(s-\tau)'\mathbf{c}|\boldsymbol{\theta}\right]^2 \Big|_{s=t_{jm}}\right)\right)\right\}. \end{aligned} \quad (9)$$

We conduct a random walk MH with a Gaussian kernel to propose τ .

1. $\tau^* \sim N(\tau^{(n)}, \sigma_\tau^2)$,
2. compute the acceptance probability

$$p_{MH} = \min\left\{1, \frac{\gamma_r(\tau^*|\mathbf{c}, \boldsymbol{\theta}, \lambda)}{\gamma_r(\tau^{(n)}|\mathbf{c}, \boldsymbol{\theta}, \lambda)}\right\},$$

3. sample $u \sim U(0, 1)$, we accept $\tau^{(n+1)} = \tau^*$ if $u < p_{MH}$, otherwise we set $\tau^{(n+1)} = \tau^{(n)}$.

- The existence of closed-form conditional posterior distributions $\pi_r(\theta_d|\mathbf{c}, \tau, \lambda)$ and $\pi_r(\mathbf{c}_i|\boldsymbol{\theta}, \boldsymbol{\sigma}, \mathbf{c}_{-i}, \lambda)$ depends on g_i ($i = 1, 2, \dots, I$). If all g_i are linear functions of θ_d (or \mathbf{c}_i), there exists closed-form conditional posterior distribution $\pi_r(\theta_d|\mathbf{c}, \tau, \lambda)$ (or $\pi_r(\mathbf{c}_i|\boldsymbol{\theta}, \boldsymbol{\sigma}, \mathbf{c}_{-i}, \lambda)$), which is Gaussian distributed. Otherwise, we conduct a random walk MH algorithm with a Gaussian kernel.
- If the conditional distribution $\pi_r(\mathbf{c}_i|\tau, \boldsymbol{\theta}, \boldsymbol{\sigma}, \mathbf{c}_{-i}, \lambda)$ does not admit a closed form. We conduct a random walk MH with a Gaussian kernel with

$$\begin{aligned} \gamma_r(\mathbf{c}_i|\tau, \boldsymbol{\theta}, \boldsymbol{\sigma}, \mathbf{c}_{-i}, \lambda) &\propto \\ \exp\left\{-\alpha_r \sum_{i=1}^I \sum_{j=1}^J \left(\frac{(y_{ij} - \boldsymbol{\Phi}(t_{ij})'\mathbf{c}_i)^2}{2\sigma_i^2} + \frac{\lambda}{2} \sum_{m=1}^M v_{jm} \cdot \left(\left[\frac{d\boldsymbol{\Phi}(s)'}{ds} \mathbf{c}_i - g_i(\boldsymbol{\Phi}(s)'\mathbf{c}, \boldsymbol{\Phi}(s-\tau)'\mathbf{c}|\boldsymbol{\theta})\right]^2 \Big|_{s=t_{jm}}\right)\right)\right\} \end{aligned}$$

- If the conditional distribution $\pi_r(\boldsymbol{\theta}|\mathbf{c}, \tau, \lambda)$ does not admit a closed form. We conduct a random walk MH with a Gaussian kernel with

$$\gamma_r(\boldsymbol{\theta}|\mathbf{c}, \tau, \lambda) \propto \exp \left\{ -\alpha_r \sum_{i=1}^I \sum_{j=1}^J \left(\frac{\lambda}{2} \sum_{m=1}^M v_{jm} \cdot \left[\frac{d\boldsymbol{\Phi}(s)'}{ds} \mathbf{c}_i - g_i(\boldsymbol{\Phi}(s)'\mathbf{c}, \boldsymbol{\Phi}(s-\tau)'\mathbf{c}|\boldsymbol{\theta}) \right] \Big|_{s=t_{jm}} \right) \right\}. \quad (11)$$

- The conditional posterior distribution of λ is $Gamma(a_\lambda + \alpha_r \sum_{i=1}^I (L_i - 2)/2, b_{\lambda^*})$, where

$$\frac{1}{b_{\lambda^*}} = \frac{1}{b_\lambda} + \frac{\alpha_r}{2} \sum_{i=1}^I \sum_{j=1}^J \sum_{m=1}^M v_m \cdot \left[\frac{d\boldsymbol{\Phi}(s)'}{ds} \mathbf{c}_i - g_i(\boldsymbol{\Phi}(s)'\mathbf{c}, \boldsymbol{\Phi}(s-\tau)'\mathbf{c}|\boldsymbol{\theta}) \right] \Big|_{s=t_{jm}}.$$

Step 3. We conduct a resampling step to prune particles with small weights. The particles after the resampling step are denoted by $\{\tilde{\boldsymbol{\beta}}_{k,r}\}_{k=1,\dots,K}$, and all particles are equally weighted. The simplest resampling method is multinomial resampling based on the normalized particle weights. However, advanced resampling schemes such as stratified resampling (Hol et al., 2006), residual resampling (Douc and Cappé, 2005) are more preferable than multinomial resampling, since multinomial resampling will create more variance for the SMC estimator compared with advanced resampling algorithms. In our numerical experiments, we use systematic resampling.

It is not recommended to conduct resampling at every iteration as resampling will create additional variation to the estimator (Chopin et al., 2004). Our resampling scheme is typically triggered when the effective sample size (ESS) falls below a given threshold ϵ . The ESS at iteration r can be computed by

$$ESS_{K,r} = \frac{1}{\sum_{k=1}^K (W_{k,r})^2}.$$

$ESS_{K,r}$ denotes the number of “perfect” samples used to approximate the intermediate distribution π_r . Effective sample size takes value between 1 and K . It takes value K if all particles are equally weighted, and it takes value that is close to 1 if one of particles has a much larger weight compared with the rest. If we never conduct resampling, the annealed SMC algorithm degenerates to the annealed importance sampling (Neal, 2001).

After conducting the annealed SMC algorithm, we obtain a list of weighted samples to empirically represent the posterior distribution $\pi(\boldsymbol{\beta})$,

$$\hat{\pi}(\boldsymbol{\beta}) = \sum_{k=1}^K W_{k,R} \cdot \delta_{\boldsymbol{\beta}_{k,R}}(\boldsymbol{\beta}).$$

3.2 Properties of the annealed SMC algorithm

We discuss some properties of our annealed SMC method. First, our annealed SMC method can provide consistency representation of intermediate target posterior distributions. This is illustrated by the following *Proposition 1*.

Proposition 1. For $K > 1$, the annealed SMC method provides asymptotically consistent estimates. We have

$$\sum_{k=1}^K W_{k,r} \psi(\boldsymbol{\beta}_{k,r}) \rightarrow \int \pi_r(\boldsymbol{\beta}) \psi(\boldsymbol{\beta}) d\boldsymbol{\beta} \quad \text{as } K \rightarrow \infty,$$

where the convergence is in L^2 norm, and ψ is a target function that satisfies regularity conditions, for example ψ is bounded. Del Moral (2004) and Chopin et al. (2004) discussed more general conditions which include the case of our annealed SMC algorithm.

Proposition 2 shows the central limit theorem, which can be used to assess the total variance of Monte Carlo estimators.

Proposition 2. Under the integrability conditions given in Theorem 1 of Chopin et al. (2004), or Del Moral (2004), pages 300 – 306 in Section 9.4,

$$K^{1/2} \left[\sum_{k=1}^K W_{k,r} \psi(\boldsymbol{\beta}_{k,r}) - \int \pi_r(\boldsymbol{\beta}) \psi(\boldsymbol{\beta}) d\boldsymbol{\beta} \right] \rightarrow N(0, \sigma_r^2(\psi)) \quad \text{as } K \rightarrow \infty,$$

where the convergence is in distribution. The form of asymptotic variance $\sigma_r^2(\psi)$ depends on the resampling scheme, the Markov kernel K_r and the artificial backward kernel L_r . We refer readers to Del Moral et al. (2006) for details of this asymptotic variance.

The second advantage of our SMC method is that it can provide an unbiased marginal likelihood estimator, with a fixed sequence of annealing parameters.

Proposition 3. For fixed $0 = \alpha_0 < \alpha_1 < \dots < \alpha_R = 1$, $\hat{Z}_{K,R} = \prod_{r=1}^R (\sum_{k=1}^K W_{k,r-1} \cdot \tilde{w}_{k,r})$ is an unbiased estimator of Z ,

$$E(\hat{Z}_{K,R}) = Z.$$

This is a well known property of SMC methods (*Theorem 7.4.2* of Del Moral (2004)). This unbiased marginal likelihood estimate $\hat{Z}_{K,R}$ is based on the unnormalized importance weights from all iterations of the SMC, which can be computed without extra cost. The computation for the marginal likelihood of MCMC based methods are generally challenging, and the unbiasedness

property depends on the convergence of powered MCMC chains, which is difficult to assess in reality.

In addition, the annealed SMC algorithm can be easily parallelized, by allocating particles across different cores.

3.3 Adaptive annealing parameter scheme in SMC

In the annealed SMC algorithm, one challenge is to properly select the sequence of annealing parameters. If we choose $\alpha_0 = 0$ and $\alpha_1 = 1$, the annealed SMC degenerates to importance sampling. A large number of annealing parameters improves the performance of algorithm, but it will be computationally more intensive. If we select an insufficient number of annealing parameters or an improper annealing scheme, the algorithm may collapse. We propose an adaptive annealing parameter scheme based on the seminar work of Del Moral et al. (2012); Zhou et al. (2016); Wang et al. (2019). Note that the weight function (Equation 7) for iteration r only depends on particles of the $(r-1)$ -th iteration, and the difference between two successive annealing parameters $\alpha_r - \alpha_{r-1}$. This indicates that we can “manipulate” $\tilde{w}_{r,k}$ by changing the annealing parameter α_r . If α_r is close to α_{r-1} , the incremental weight function $\tilde{w}_{k,r} = p(\mathbf{y}|\tilde{\boldsymbol{\beta}}_{k,r-1})^{\alpha_r - \alpha_{r-1}}$ is close to 1, and the variance of $\tilde{w}_{k,r}$ is smaller than it would be if we chose a larger value of α_r . This provides the intuition that we are able to control the discrepancy between two successive intermediate target distributions by manipulating α_r .

In this article, we use the relative conditional effective sample size (rCESS) (Zhou et al., 2016) to measure the discrepancy between two successive intermediate targets. The rCESS is defined as

$$\text{rCESS}_r(W_{\cdot,r-1}, \tilde{w}_{\cdot,r}) = \frac{\left(\sum_{k=1}^K W_{k,r-1} \tilde{w}_{k,r}\right)^2}{\sum_{k=1}^K W_{k,r-1} (\tilde{w}_{k,r})^2},$$

which takes a value between $1/K$ and 1. The rCESS is equal to the relative ESS if we conduct resampling at every SMC iteration. Using the fact that $\tilde{w}_{k,r} = p(\mathbf{y}|\boldsymbol{\beta}_{k,r-1})^{\alpha_r - \alpha_{r-1}}$, rCESS_r is a decreasing function of α_r , where $\alpha_r \in (\alpha_{r-1}, 1]$. We control rCESS over iterations by selecting the annealing parameter α such that

$$f(\alpha) = \text{rCESS}(W_{\cdot,r-1}, p(\mathbf{y}|\boldsymbol{\beta}_{\cdot,r-1})^{\alpha - \alpha_{r-1}}) = \phi,$$

where ϕ is a value between 0 and 1. A small value of ϕ will lead to a high value of α_r , while a large value of ϕ will lead to a low value of α_r . It is impossible to obtain a closed-form solution of

α^* by solving $f(\alpha) = \phi$, but we are able to use a bisection method to solve this one-dimensional search problem. The search interval of α is $(\alpha_{r-1}, 1]$. By using $f(\alpha_{r-1}) - \phi > 0$, $f(1) - \phi < 0$ (in case $f(1) \geq \phi$, we set $\alpha_r = 1$), and the continuous property of $f(\alpha) - \phi$, the solution α^* of $f(\alpha) = \phi$ is guaranteed. Algorithm 1 provides a detailed description for the SMC algorithm.

Algorithm 1 An SMC algorithm of Bayesian inference for parameters in DEs

- 1: **Inputs:** (a) Priors π_0 over model parameters β , where $\beta = (\theta, \tau, \mathbf{c}, \sigma, \lambda)'$; (b) relative CESS $\{\phi_r\}_{r=1, \dots, R}$; (c) resampling threshold ϵ .
- 2: **Outputs:** (a) Posterior approximation, $\hat{\pi}(\beta) = \sum_{k=1}^K W_{k,R} \cdot \delta_{\beta_{k,R}}(\beta)$; (b) marginal likelihood estimates \hat{Z}_R .
- 3: Initialize SMC iteration index and annealing parameter: $r \leftarrow 0$, $\alpha_0 \leftarrow 0$.
- 4: Initialize the marginal likelihood estimate $\hat{Z}_0 \leftarrow 1$.
- 5: **for** $k \in \{1, 2, \dots, K\}$ **do**
- 6: Initialize particles with independent samples: $\beta_{k,0} \leftarrow (\theta_{k,0}, \tau_{k,0}, \mathbf{c}_{k,0}, \sigma_{k,0}, \lambda_{k,0})'$.
- 7: Initialize weights to unity: $w_{0,k} \leftarrow 1$, $W_{0,k} \leftarrow 1/K$.
- 8: **for** $r \in \{1, 2, \dots\}$ **do**
- 9: Compute annealing parameter α_r using bisection method with

$$f(\alpha) = \text{rCESS}(W_{\cdot, r-1}, p(\mathbf{y}|\beta_{\cdot, r-1})^{\alpha - \alpha_{r-1}}) = \phi_r.$$

- 10: **for** $k \in \{1, \dots, K\}$ **do**
 - 11: Compute unnormalized weights for $\beta_{k,r}$: $w_{k,r} = w_{k,r-1} \cdot [p(\mathbf{y}|\tilde{\beta}_{k,r-1})]^{\alpha_r - \alpha_{r-1}}$.
 - 12: Normalize weights: $W_{k,r} = w_{k,r} / (\sum_{k=1}^K w_{k,r})$.
 - 13: Sample particles $\beta_{k,r}$ with one MCMC move admitting π_r as stationary (shown in Eq (8-10)).
 - 14: Update marginal likelihood estimate $\hat{Z}_r = \hat{Z}_{r-1} \cdot \sum_{k=1}^K W_{k,r-1} \tilde{w}_{k,r}$.
 - 15: **if** $\phi_r = 1$ **then**
 - 16: return the current particle population $(\beta_{k,r}, W_{k,r})_{k=1, \dots, K}$.
 - 17: **else**
 - 18: **if** $\text{rESS} < \epsilon$ **then**
 - 19: Resample the particles.
 - 20: **for** $k \in \{1, \dots, K\}$ **do**
 - 21: Reset particle weights: $w_{k,r} = 1$, $W_{k,r} = 1/K$.
 - 22: **else**
 - 23: **for** $k \in \{1, \dots, K\}$ **do**
 - 24: $\tilde{\beta}_{k,r} = \beta_{k,r}$.
-

4 Real Data Analysis

In the dynamic system of the blowfly population, resource limitation acts with a time delay, roughly equal to the time for an egg to grow up to a pupa. Figure 3 displays the counts of blowflies over

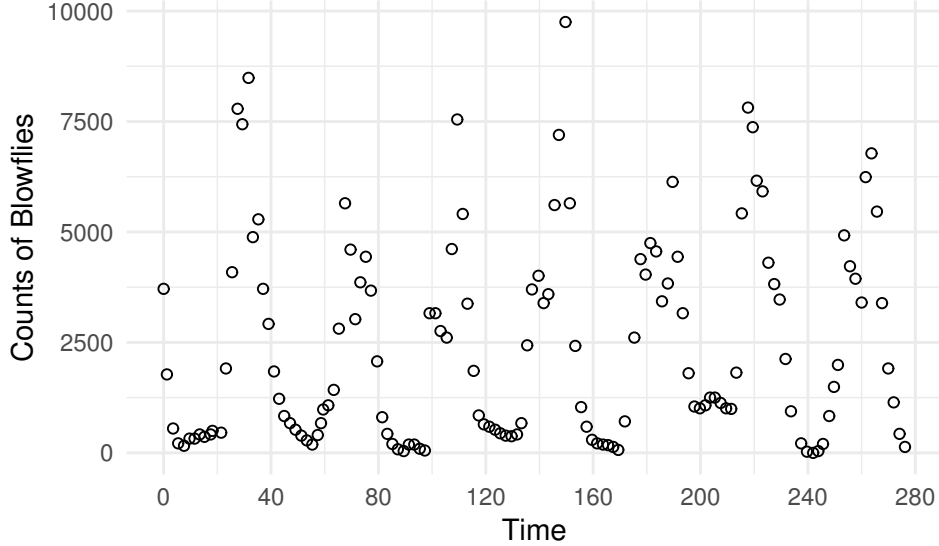


Figure 3: Blowfly population in one experiment published in Nicholson (1954); the time unit is one day.

time studied in Nicholson (1954). The time unit is one day. The oscillations displayed in blowfly population is caused by the time lag between stimulus and reaction (Berezansky et al., 2010). May (1976) proposed to model the counts of blowflies with the following DDE model

$$\frac{dx(t)}{dt} = \nu x(t)[1 - x(t - \tau)/(1000 \cdot P)], \quad (12)$$

where $x(t)$ is the blowfly population, ν is the rate of increase of the blowfly population, P is a resource limitation parameter set by the supply of food, and τ is the time delay, roughly equal to the time for an egg to grow up to a pupa. Our goal is to estimate the initial value, $x(0)$, and the three parameters, ν , P , and τ , from the noisy Nicholson's blowfly data $y(t)$. The observed counts of blowflies $y(t)$ is assumed to be lognormal distributed with mean $x(t)$ and variance σ^2 .

The counts of blowfly $x(t)$ is a positive function. Instead of modelling the constrained function $x(t)$ by a linear combination of cubic B-spline basis functions $x(t) = \Phi(t)'c_i$, we transform $x(t) = e^{W(t)}$ and use B-spline basis functions to model the unconstrained function $W(t) = \Phi(t)'c_i$, equivalently we solve delay differential equation

$$\frac{dW(t)}{dt} = \nu[1 - e^{W(t-\tau)}/(1000 \cdot P)], \quad (13)$$

with noisy observations $\log y(t) \sim N(W(t), \sigma^2)$.

We approximate the DDE solution using cubic B-splines with 34 equally spaced interior knots over the time span. The total number of knots is equal to 36. The total number of cubic B-spline functions is $L = 38$. Selection of the number of basis functions will be explored in Section 5.1.3. Our prior distributions for parameter of interest $(\mathbf{c}, \nu, P, \tau, \sigma^2)'$ are

$$\begin{aligned} \nu &\sim N(0, 5^2)I(\nu > 0), & P &\sim N(0, 5^2)I(P > 0), & \tau &\sim Unif(0, 50), \\ \mathbf{c} &\sim MVN(\mathbf{0}_L, 100^2\mathbf{I}_L), & \sigma^2 &\sim IG(1, 1), & \lambda &\sim Gamma(1, 1). \end{aligned}$$

In our adaptive SMC, we set $rCESS = 0.9$ and resampling threshold $\epsilon = 0.5$. The number of particles is $K = 500$. Under this setting, the number of SMC iteration $R = 227$. In Section 5.1.2, we will compare the performance of our method using different values of $rCESS$ and K . Figure 4 displays the estimated DDE trajectory. The left panel of Figure 4 shows the estimated $W(t)$ and the 95% credible bands; the right panel of Figure 4 shows $X(t) = e^{W(t)}$, in which the blue points are observed data.

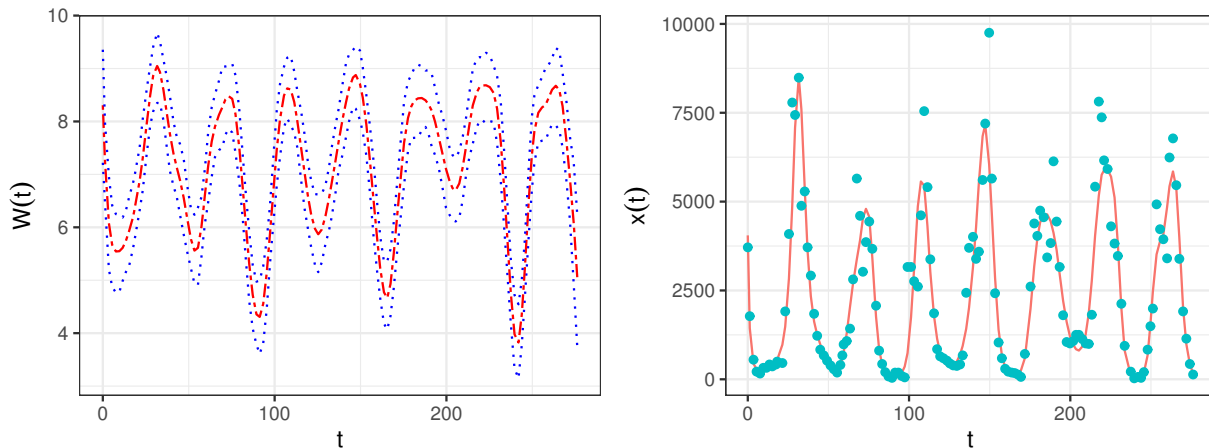


Figure 4: Estimated posterior mean trajectory and 95% credible bands for the delay differential equation modelling the population dynamics of blowflies.

Table 3 displays the posterior means and the corresponding 95% credible intervals (CI) for DDE parameters in Equation (13). Note that our point estimates are similar to those obtained from Wang and Cao (2012), in which the same nonparametric function expressed using B-splines is estimated by maximizing the DDE-defined penalized likelihood function. However, the uncertainty of these parameters is significantly underestimated using their frequentist approach. In contrast, our Bayesian approach can provide more reasonable estimates for the parameter uncertainty. More

concretely, we compare the estimates for the main parameter of interest, the delay parameter τ , which can be interpreted as the time for an egg to grow up to a pupa. From Table 3, our posterior mean of τ and its 95% CI is 8.368 (5.656, 9.916) while the maximum likelihood estimate for τ is 8.781 and the standard error is 0.039 in Wang and Cao (2012).

Figure 5 displays the pairwise scatter plots of the posterior samples of ν , τ and P . We also calculate the correlation between posterior samples: $\text{corr}(\nu, \tau) = 0.139$, $\text{corr}(\nu, P) = 0.598$, $\text{corr}(P, \tau) = 0.008$. Recall that ν is the rate of increase of the blowfly population and τ is the time delay, roughly equal to the time for an egg to grow up to a pupa. The small positive value of the correlation between τ and ν indicates that the blowfly population will increase if eggs take their time to well develop to pupas. The parameter P is related to a resource limitation. The relative large positive correlation between ν and P can be easily understood: the blowfly population grows faster when there is a larger food supply. The tiny positive value of the correlation between τ and P implies that the amount of food supply has a small impact on the period of being a pupa.

Table 1: Posterior mean and corresponding 95% credible interval (CI) for parameters in population dynamics of blowflies.

	ν	P	τ
Mean	0.176	2.372	8.368
(2.5%, 97.5%)	(0.074, 0.284)	(1.307, 3.333)	(5.656, 9.916)
	$W(0)$	σ^2	λ
Mean	8.299	0.527	3.348
(2.5%, 97.5%)	(7.220, 9.355)	(0.460, 0.607)	(1.633, 5.910)

5 Simulation Study

We use simulation studies to demonstrate the effectiveness of our proposed model and method. The experiments include both ODE and DDE examples. We use the R package *deSolve* (Soetaert et al., 2010) to simulate differential equations.

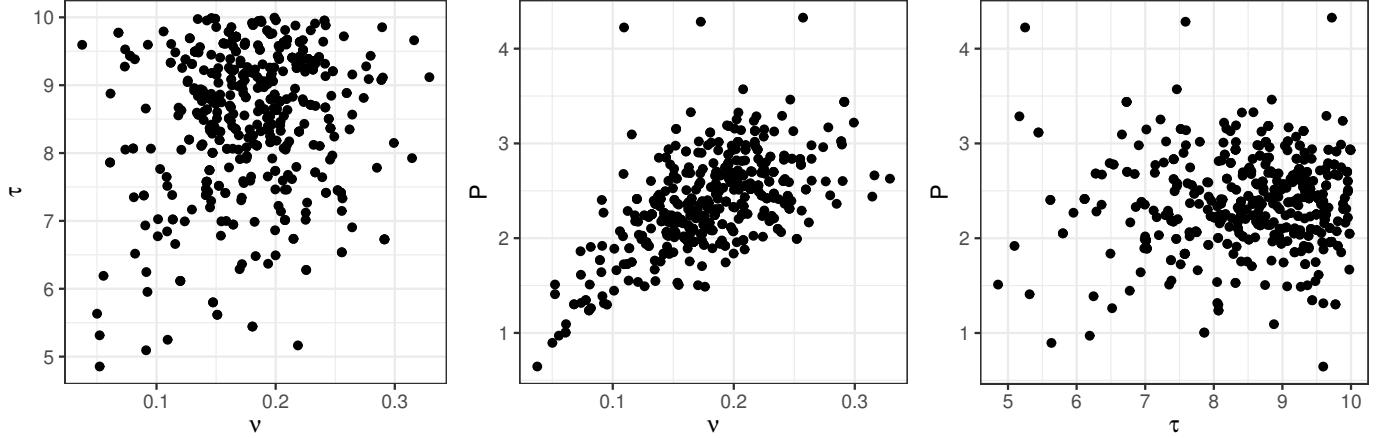


Figure 5: Posterior samples of ν , τ , P for DDE in Equation (13) estimated via SMC. We re-sample the particles at the last SMC iteration such that they are equally weighted. Correlation: $\text{corr}(\nu, \tau) = 0.139$, $\text{corr}(\nu, P) = 0.598$, $\text{corr}(P, \tau) = 0.008$.

5.1 A nonlinear ordinary differential equation example

In this section, we use a nonlinear ODE example to illustrate the numerical behaviour of SMC algorithm. We generate ODE trajectories according to the following ODE system,

$$\begin{aligned} \frac{dx_1(t)}{dt} &= \frac{72}{36 + x_2(t)} - \theta_1, \\ \frac{dx_2(t)}{dt} &= \theta_2 x_1(t) - 1, \end{aligned} \quad (14)$$

where $\theta_1 = 2$ and $\theta_2 = 1$, and initial conditions $x_1(0) = 7$ and $x_2(0) = -10$. The observations \mathbf{y}_i are simulated from a normal distribution with mean $x_i(t|\boldsymbol{\theta})$ and variance σ_i^2 , where $\sigma_1 = 1$ and $\sigma_2 = 3$. We generate 121 observations for each ODE function, equally spaced within $[0, 60]$ (see Figure 6). Under this setting, the posterior distribution of θ_1 and θ_2 will have multiple local modes (see Figure 1).

We use cubic B-spline functions (see Figure 2) to represent ODE trajectories. We put equally spaced knots on each of eight observations. The total number of knots is 16, including 14 interior knots. The total number of cubic B-spline functions is $L = 18$. We select weak prior distributions

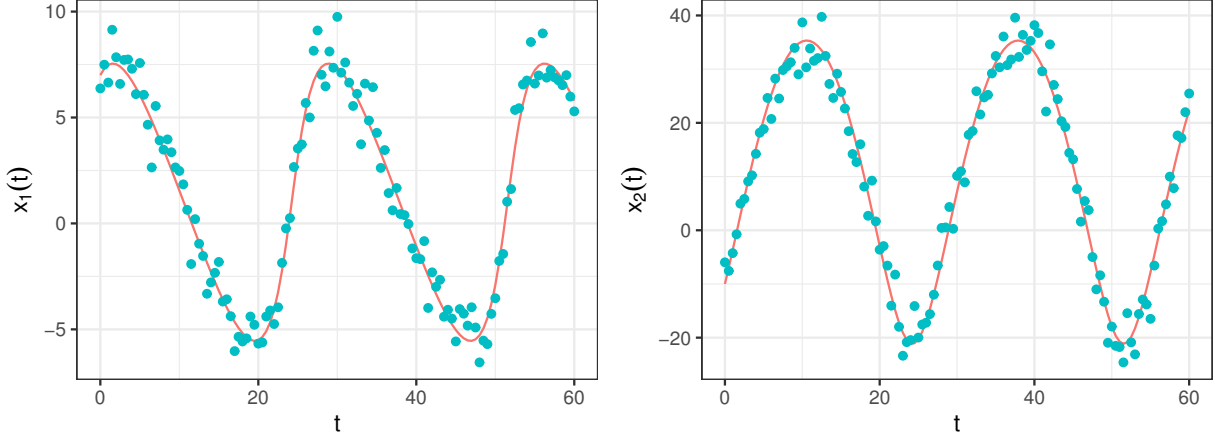


Figure 6: Simulated ODE trajectories and observations. Red lines in the figure refer to simulated ODE trajectories and blue points refer to simulated observations.

of β for the SMC algorithm,

$$\begin{aligned}
 \theta_1 &\sim N(5, 5^2), & \theta_2 &\sim N(5, 5^2), \\
 \mathbf{c}_1 &\sim MVN(\mathbf{0}_L, 100^2 \mathbf{I}_L), & \mathbf{c}_2 &\sim MVN(\mathbf{0}_L, 100^2 \mathbf{I}_L), \\
 \sigma_1^2 &\sim IG(1, 1), & \sigma_2^2 &\sim IG(1, 1), & \lambda &\sim Gamma(1, 1).
 \end{aligned}$$

5.1.1 One bimodal example

We first alter Equation (14) to produce a symmetric, bimodal posterior for θ_1 ,

$$\begin{aligned}
 \frac{dx_1(t)}{dt} &= \frac{72}{36 + x_2(t)} - |\theta_1|, \\
 \frac{dx_2(t)}{dt} &= \theta_2 x_1(t) - 1.
 \end{aligned} \tag{15}$$

In our adaptive SMC, we set rCESS = 0.9 and resampling threshold $\epsilon = 0.5$. The total number of particles we use is $K = 500$. Under this setting, the number of annealing parameters is 752. We show the approximated intermediate posterior distributions for θ and σ when $r = 1$ (grey points), 50 (orange points), 300 (light blue points) and 752 (dark blue points) (see two panels in the first row of Figure 7). With the increment of annealing parameters, the particles gradually move to the posterior distribution. We create two main modes for θ_1 in Equation (15). The SMC algorithm is able to find these two global modes of θ_1 while avoiding being stuck in local modes. We reported the estimated ODE trajectories and the 95% credible bands in the two bottom panels of Figure

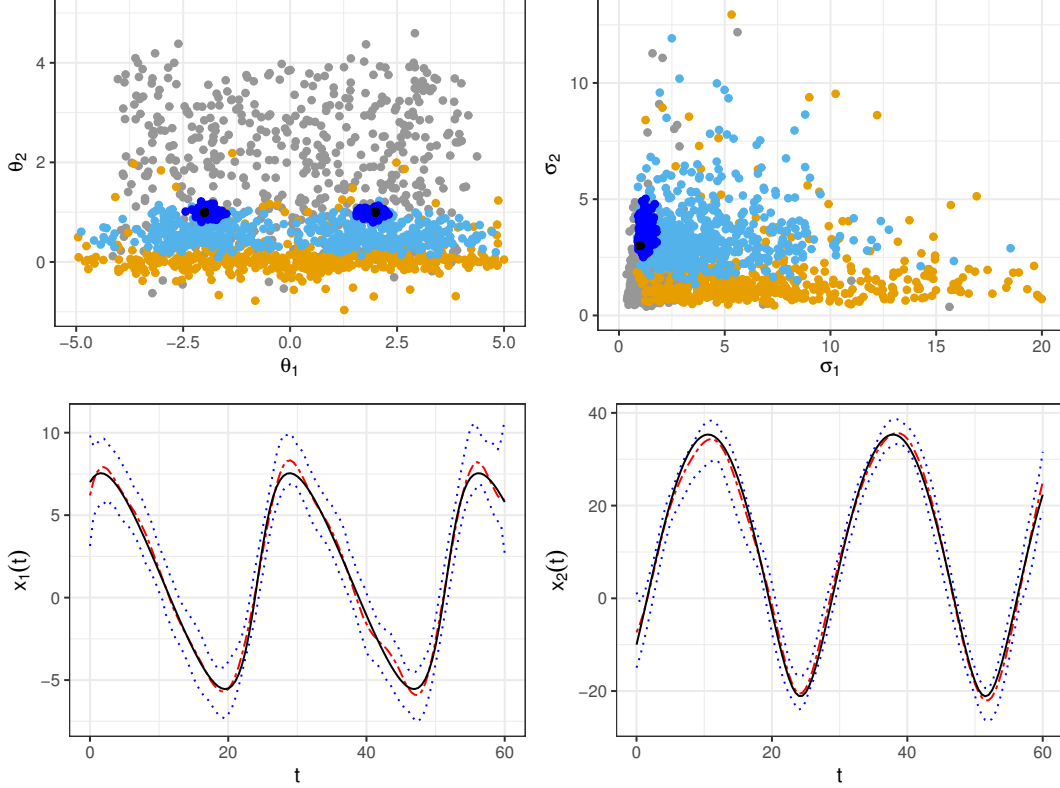


Figure 7: Intermediate posterior distributions for $\boldsymbol{\theta}$ and $\boldsymbol{\sigma}$ (two panels in the first row, grey, orange, light blue and dark blue points are samples for $r = 1, 50, 300, 752$, the black dots indicate true values for generating ODE), and estimated ODE trajectories and the 95% confidence bands (two panels in the second row).

7. The estimated mean ODE trajectories are very close to the true ODE trajectories. The 95% credible bands covers the true ODE trajectories.

We compare the performance of SMC with the MCMC illustrated in Appendix. With given samples $\boldsymbol{\theta}^{(n)}$, $\mathbf{x}(0)^{(n)}$ at the n -th MCMC iteration, we use *deSolve* (Soetaert et al., 2010) to solve ODEs, to obtain $\mathbf{x}(t_{ij}|\boldsymbol{\theta}^{(n)}, \mathbf{x}(0)^{(n)})$. We select weak prior distributions for $\boldsymbol{\theta}$ and $\mathbf{x}(0)$. We run an MCMC algorithm with 400,000 iterations, which is close to $K \cdot R$ in SMC. The acceptance rate of MH algorithm is 25.2%. Figure 8 displays the MCMC trace plots of $\boldsymbol{\theta}$. It indicates that MCMC is getting stuck in local modes close to the initial value, and cannot explore the two main modes created in Equation (15).

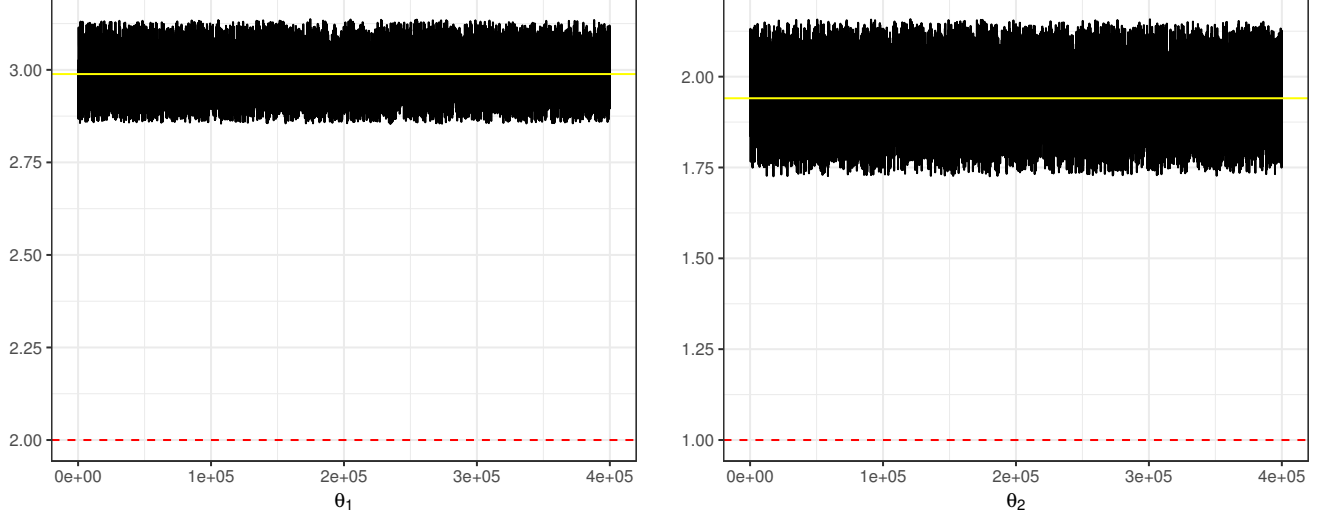


Figure 8: MCMC traceplot for θ . The yellow line denotes the posterior mean, and the red dashed line denotes the true value of θ .

5.1.2 Comparison of using different rCESS and K

We conduct experiments to investigate the performance of the SMC algorithm with different thresholds of rCESS and K using the ODE system showed in Equation (14). We simulate 20 datasets according to *Section 5.1*. We compare the performance of the SMC algorithm in terms of estimated θ , σ and estimated ODE. With estimated basis coefficients $\hat{\mathbf{c}}_i$, we are able to compute the estimated i -th ODE trajectory $\hat{x}_i(t) = \Phi(t)' \hat{\mathbf{c}}_i$. We define the distance between the estimated i -th ODE trajectory $\hat{x}_i(t)$ and the true ODE $x_i(t)$ that we use to simulate data as

$$\text{RMSE}(x_i(t)) = \left[\frac{1}{J} \sum_{j=1}^J (\Phi(t_{ij})' \hat{\mathbf{c}}_i - x_i(t_{ij}))^2 \right]^{1/2}. \quad (16)$$

We select three different levels of rCESS (rCESS = 0.8, 0.9, 0.99). We put equally spaced interior knots on each of the 12 observations. The total number of basis function is 13. The number of particles we use is $K = 500$. For each level of rCESS, we run the SMC algorithm 20 times (once for each dataset). Figure 9 displays boxplots of the posterior samples of θ , σ and $\text{RMSE}(x_i(t))$ from SMC with different rCESS thresholds. It indicates that the parameter estimates get closer to the true values, and RMSE of the ODE trajectories gets smaller, when we increase the rCESS threshold. A higher value of rCESS threshold is equivalent to more intermediate target distributions.

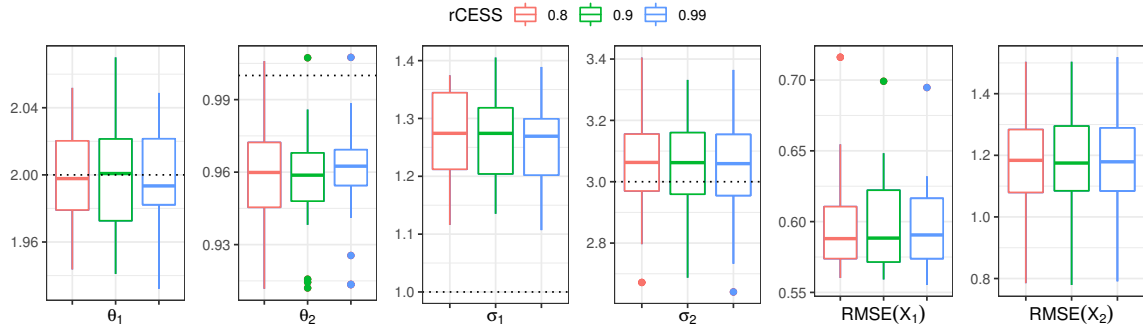


Figure 9: ODE parameter estimates with different rCESS in SMC.

We select three different levels of K ($K = 10, 100, 2000$). We also put equally spaced interior knots and the total number of basis function is 13. We set $\text{rCESS} = 0.9$. For each level of K , we run the SMC algorithm 20 times (once for each dataset). Figure 10 displays boxplots for θ , σ and $\text{RMSE}(x_i(t))$ from SMC with different levels of K . It indicates that the proposed SMC method performs better when we use a large number of particles. The consistency of the SMC algorithm holds when the number of particles goes to infinity (Chopin et al., 2004; Wang et al., 2019; Del Moral et al., 2006). However, we cannot use an arbitrarily large value of K as the computational cost of the SMC algorithm is a linear function of K . We recommend increasing rCESS in the SMC (using a larger number of intermediate distributions R), as increasing R does not increase the memory burden.

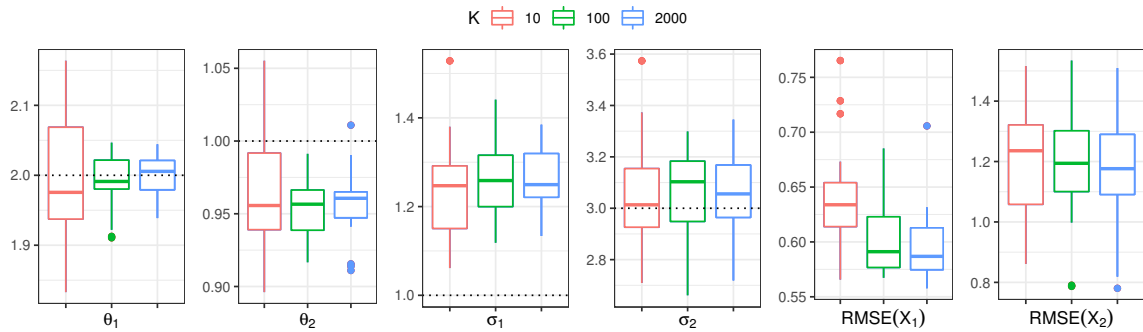


Figure 10: Boxplots for ODE parameter estimates with different values of K in SMC.

5.1.3 Number of basis functions and selection of λ

In this section, we first conduct experiments to investigate the performance of the SMC algorithm with different numbers of basis functions in terms of estimating θ , σ and the RMSE of the estimated ODE trajectories. The knots for basis function are equally spaced. We choose five different numbers of basis function, $\text{nbasis} = 7, 11, 16, 31, 61$. We set $K = 500$ and $\text{rCESS} = 0.9$ for the SMC algorithm. For each level of number of basis function, we run the SMC once for each of the 20 datasets simulated in *Section 5.1.2*. Figure 11 displays the ODE parameter estimates with different numbers of basis functions. The parameter estimates θ and σ get closer to true values, and the RMSE values of estimated ODE trajectories decrease if we increase the number of basis functions from 7 to 16. However, the parameter estimates and RMSE of the estimated ODE trajectories become worse if we use a large number of basis functions. This experiment indicates a sufficient number of basis functions is important in ODE trajectory estimation. However, we do not recommend using a overly large number of basis functions as it will cause over fitting and induce a heavy computational cost.

The second experiment we conduct is a comparison between the performance of the SMC algorithm with different choice of λ ($\lambda = 0.1, 1, 10, 100$) and the full Bayesian (FB) scheme. We put equally spaced knots and set the number of basis functions to 16. We set $K = 500$ and $\text{rCESS} = 0.9$ for the SMC algorithm. For each choice of λ , we run the SMC algorithm with one replicate for the 20 datasets simulated in *Section 5.1.2*. Figure 12 displays the ODE parameter estimates with different choices of λ . The fully Bayesian scheme performs satisfactorily in terms of parameter estimates and RMSE of the ODE trajectories. Figure 13 displays the posterior samples of λ for one SMC replicate.

5.2 Delay differential equation examples

5.2.1 Hutchinson's equation

Our first DDE example is the Hutchinson's equation, which is used to model the blowfly data in *Section 4*,

$$\frac{dx(t)}{dt} = \nu x(t)[1 - x(t - \tau)/(1000 \cdot P)],$$

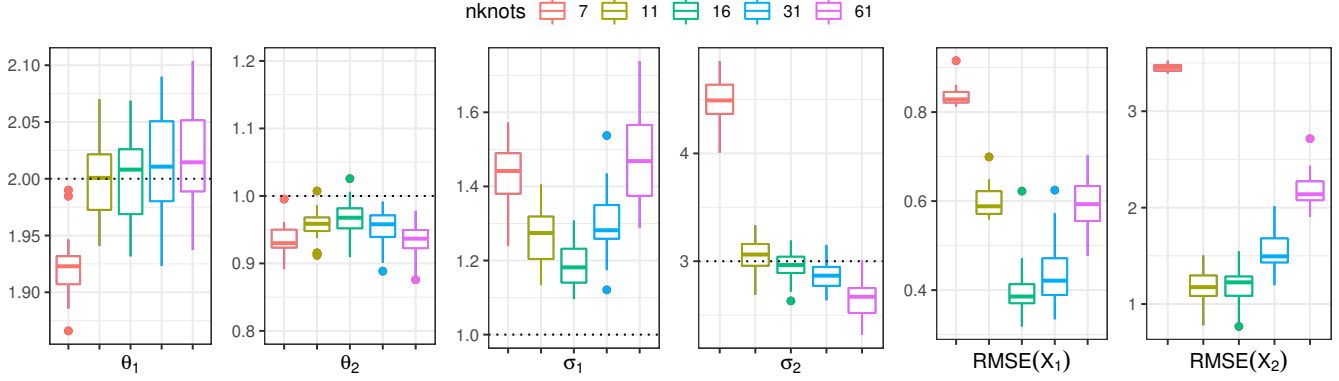


Figure 11: ODE parameter estimates obtained from SMC with different numbers of knots.

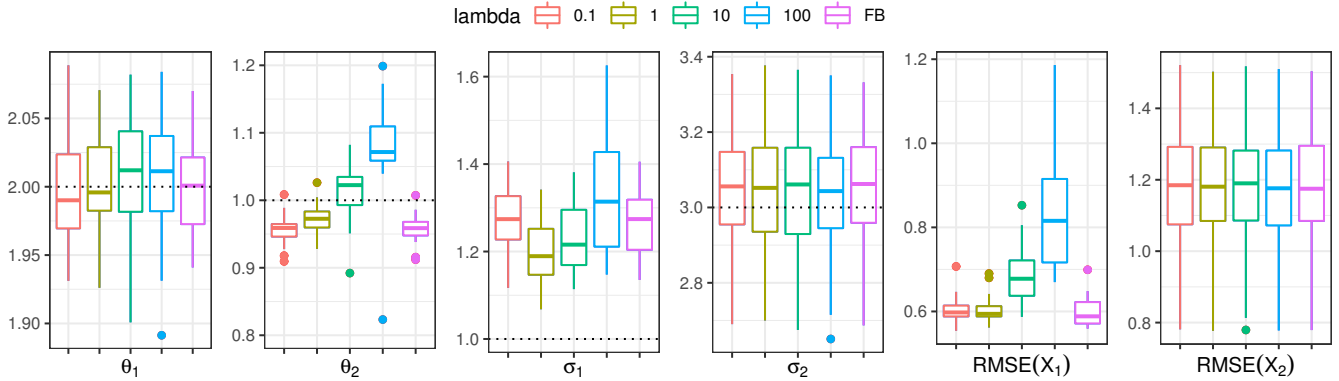


Figure 12: ODE parameter estimates with different choices of λ .

where τ , ν and P are parameters of interest in the DDE. We set $x(0) = 3500$, $\tau = 3$, $\nu = 0.8$ and $P = 2$ to simulate the DDE trajectory. The DDE trajectory is observed with measurement error. The error is lognormal distributed with mean 0 and standard deviation $\sigma = 0.4$. We simulate 3 data sets, with 101, 201 and 401 observations respectively, equally spaced in $[0, 100]$.

We transform the positive constraint function $x(t) = e^{W(t)}$ and use B-spline basis functions to model the unconstrained one $W(t) = \Phi(t)'c_i$. This is equivalent to solving the delay differential equation displayed in Equation (13). We put 51 knots equally spaced in $[0, 100]$, including 49 interior knots. The total number of cubic B-spline functions is $L = 53$. The hyper-parameters in DDE parameter prior and sequential Monte Carlo setups are the same as *Section 4*. Table 2 displays the estimated parameters (ν, P, τ) and RMSE defined in Equation (16) for $W(t)$. For the same DDE function, a larger number of observations improves the performance of estimation.

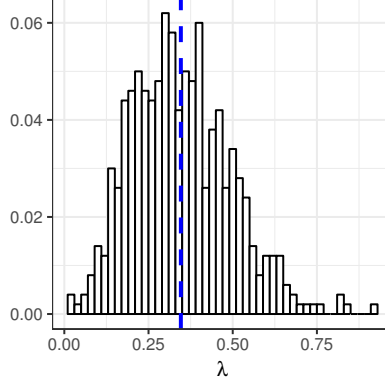


Figure 13: One example of posterior samples of λ .

5.2.2 A nonlinear delay differential equation example

In this section, we investigate a nonlinear delay differential equation model proposed by Monk (2003) to model the feedback inhibition of gene expression. The nonlinear DDE is described as follows:

$$\begin{aligned} \frac{dx_1(t)}{dt} &= \frac{1}{1 + (x_2(t - \tau)/p_0)^n} - \mu_m x_1(t), \\ \frac{dx_2(t)}{dt} &= x_1(t) - \mu_p x_2(t). \end{aligned} \quad (17)$$

In Equation (17), $x_1(t)$ denotes the expression of *mRNA* at time t , and $x_2(t)$ denotes the expression of a *protein* at time t . There is a delayed repression of *mRNA* production by the *protein*. The DDE system depends on the *transcriptional delay* τ , and degradation rates μ_m and μ_p , the expression threshold p_0 and the Hill coefficient n . As noted in Monk (2003), there is significant nonlinearity in the DDE system when the Hill coefficient $n > 4$.

We simulate a delay differential equation system with $\tau = 25$, $p_0 = 100$, $\mu_m = 0.03$, $\mu_p = 0.03$, and n is set to 8. The observations $y_i(t)$ are simulated from a normal distribution with mean $x_i(t|\boldsymbol{\theta})$ and variance σ_i^2 , where $\sigma_1 = 1$ and $\sigma_2 = 5$. We generate 101 observations for each DDE function, equally spaced in $[0, 500]$. Figure 14 represents the simulated DDE system, which exhibits oscillations in *mRNA* and *protein* expression.

We allocate equally spaced knots within $[0, 500]$. The total number of cubic B-spline basis

Table 2: Estimated parameters and MSE of $W(t)$ for three simulated data sets.

J	ν	P	τ
True	0.8	2	3
101	0.639 (0.429, 0.817)	2.072 (1.564, 2.607)	3.054 (2.664, 3.560)
201	0.729 (0.600, 0.903)	1.975 (1.655, 2.320)	3.020 (2.732, 3.256)
401	0.750 (0.632, 0.863)	2.086 (1.800, 2.383)	2.997 (2.843, 3.156)
J	$W(0)$	σ^2	MSE
True	8.161	0.16	—
101	7.926 (7.343, 8.471)	0.119 (0.083, 0.184)	0.255
201	7.902 (7.529, 8.328)	0.141 (0.112, 0.179)	0.206
401	7.977 (7.569, 8.396)	0.166 (0.145, 0.193)	0.136

function is $L = 28$. We select the weak prior distributions of β for the SMC algorithm,

$$\begin{aligned} \theta_1 &\sim N(0, 5^2), & \theta_2 &\sim N(0, 5^2), & \tau &\sim Unif(0, 50), \\ \mathbf{c}_1 &\sim MVN(\mathbf{0}_L, 100^2 \mathbf{I}_L), & \mathbf{c}_2 &\sim MVN(\mathbf{0}_L, 100^2 \mathbf{I}_L), \\ \sigma_1^2 &\sim IG(1, 1), & \sigma_2^2 &\sim IG(1, 1), & \lambda &\sim Gamma(1, 1). \end{aligned}$$

In our adaptive SMC, we set rCESS = 0.9 and resampling threshold $\epsilon = 0.5$. The total number of particles we use is $K = 300$. Under this setting, the number of annealing parameters is $R = 850$. We show the parameter estimates and the corresponding 95% credible interval (CI) in Table 3. The mean of parameters are fairly close to the true values, and the 95% credible intervals cover the true values. The estimated posterior mean of λ is 0.225.

We reported the estimated DDE trajectories and the 95% credible bands in Figure 15. The estimated mean DDE trajectories are generally very close to the true DDE trajectories. The 95% confidence bands cover the true DDE trajectories.

6 Discussion

We proposed an adaptive semi-parametric Bayesian framework to solve nonlinear differential equations and estimate the DE parameters using an efficient annealed sequential Monte Carlo method.

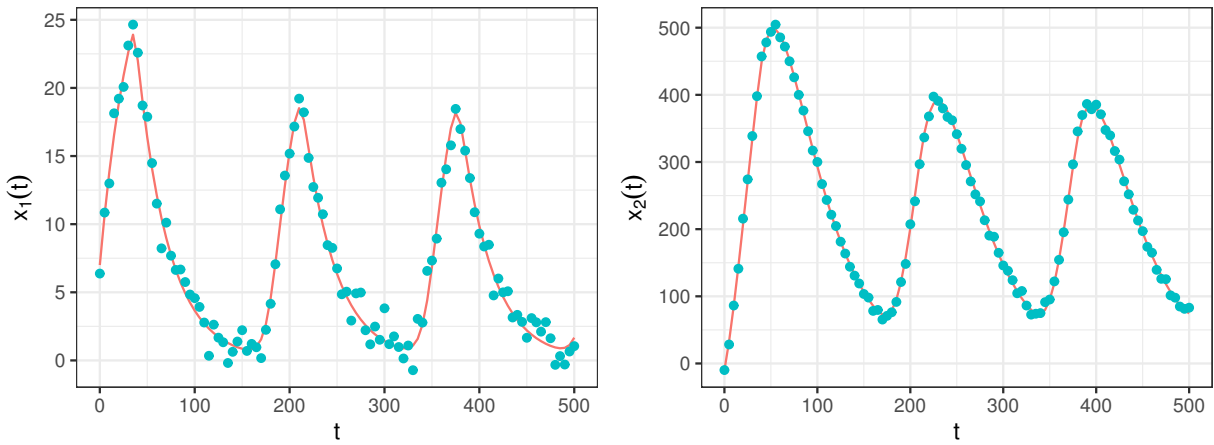


Figure 14: Simulated DDE trajectories and observations. Red lines in Figure refer to simulated DDE trajectory and blue points refer to simulated observations.

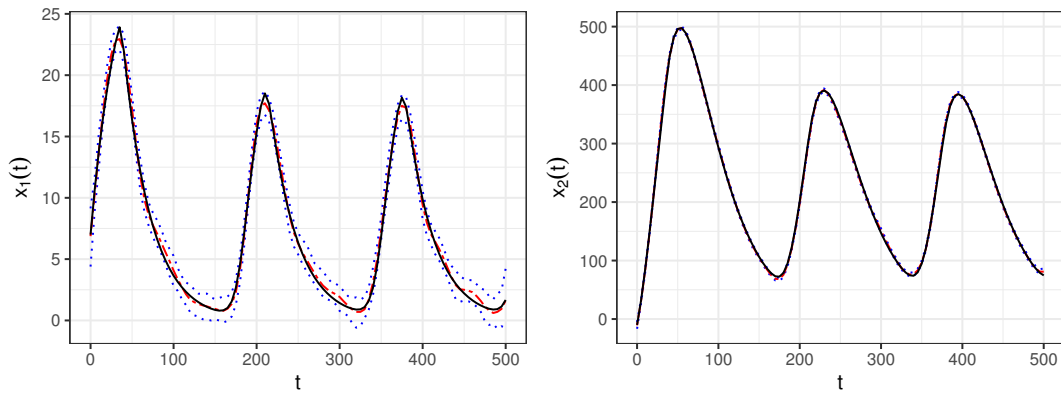


Figure 15: Estimated DDE trajectories and the 95% confidence bands using $L = 28$ basis functions.

Table 3: Parameter estimates and the corresponding 95% credible interval (CI) for nonlinear DDE models.

	True	Mean	95% CI
μ_m	0.03	0.0275	(0.0083, 0.0507)
μ_p	0.03	0.0304	(0.0294, 0.0317)
p_0	100	94.966	(68.494, 120.058)
τ	25	24.739	(12.384, 34.736)
σ_1	1	1.015	(0.872, 1.173)
σ_2	5	4.576	(4.036, 5.247)
$x_1(0)$	7	6.874	(4.392, 9.137)
$x_2(0)$	-10	-10.745	(-16.664, -5.061)

The main idea is to represent DE trajectories using a linear combination of basis functions and to estimate the coefficients of these basis functions together with other DE parameters using an annealed sequential Monte Carlo algorithm. The proposed method avoids using DE solvers which can be computationally expensive and sensitive to the initial state and model parameters. Our work is a fully Bayesian method with two obvious advantages over the counterpart using a frequent method. First, our Bayesian method can easily achieve more reasonable uncertainty estimates, illustrated by the real data analysis on the Blowfly data. Second, we avoid expensive tuning for the global smoothing parameter by treating it in the same way as other parameters.

We developed a sequential Monte Carlo in an annealing framework to estimate the model parameters. The annealed SMC considers the same parameter space for all the intermediate distributions. Consequently, the MCMC moves used in the literature on Bayesian inference for differential equations can be repurposed to act as the SMC proposal distributions in the annealed SMC. However, annealed SMC is preferred than the MCMC algorithms due to several reasons. First, the developed SMC method can fully explore the multi-modal posterior surface of DEs parameters. Second, the annealed SMC is an embarrassingly parallel method. Unlike running an MCMC chain for a super long time until it converges, the annealed SMC is more efficient because a large number of particles can be run on different CPUs or GPUs simultaneously. Third, an unbiased estimator for the marginal likelihood is readily obtained based on the unnormalized importance weights from all iterations of the SMC. The calculation of the marginal likelihood is

important for model selection but is challenging to estimate from an MCMC algorithm. Fourth, the proposed method is a semi-automatic algorithm that requires minimum tuning from the user; given a criterion for the relative conditional effective sample size and the number of particles, it can adaptively choose a scheme for the sequence of the temperature parameters that determine the intermediate target distributions of SMC.

We used different simulation scenarios to explore the numerical behavior of our model and method, and demonstrated it can perform well in both ODE and DDE parameter estimation. Our simulation studies provide some guideline for choosing the value of rCESS and the number of particles. To ensure more accurate estimates of the DE parameters from the annealed SMC, a rule of thumb is to choose a large number for rCESS and to avoid using an extremely small number of particles. We also applied our method to a real data example to model the population dynamics of blowflies with a delay differential equation. The delay parameter in DDE is usually challenging to estimate. But our application shows that our method is superior to the previous frequentist method.

There are several improvements and extensions based on our proposed method for future work. In all of our current numerical experiments, we put equally spaced knots for smoothing splines and the number of knots are pre-determined before running experiments. In future work, we will explore using a smaller number of knots that are well placed, and let the data determine the number of knots and their locations. The adaptive control of knots in smoothing spline for DEs will benefit the estimation of DEs, especially those with sharp changes. Recall that the annealed SMC can provide an unbiased estimator for the marginal likelihood. In practice, it is often the case that there are several DE models that are proposed to describe the same dynamic system. This requires selection among various differential equations models. One direction of future work is to explore model selection for DEs using the marginal likelihood obtained from the annealed SMC. Another line of future work is to develop more scalable SMC algorithms for estimating parameters in a large series of differential equations.

References

Ascher, U. M., S. J. Ruuth, and R. J. Spiteri (1997). Implicit-explicit Runge-Kutta methods for time-dependent partial differential equations. *Applied Numerical Mathematics* 25(2-3), 151–167.

- Barber, D. and Y. Wang (2014). Gaussian processes for Bayesian estimation in ordinary differential equations. In *International Conference on Machine Learning*, pp. 1485–1493.
- Berezansky, L., E. Braverman, and L. Idels (2010). Nicholson’s blowflies differential equations revisited: main results and open problems. *Applied Mathematical Modelling* 34(6), 1405–1417.
- Berry, S. M., R. J. Carroll, and D. Ruppert (2002). Bayesian smoothing and regression splines for measurement error problems. *Journal of the American Statistical Association* 97(457), 160–169.
- Bhaumik, P., S. Ghosal, et al. (2015). Bayesian two-step estimation in differential equation models. *Electronic Journal of Statistics* 9(2), 3124–3154.
- Bhaumik, P., S. Ghosal, et al. (2017). Efficient Bayesian estimation and uncertainty quantification in ordinary differential equation models. *Bernoulli* 23(4B), 3537–3570.
- Bulirsch, R. and J. Stoer (1966). Numerical treatment of ordinary differential equations by extrapolation methods. *Numerische Mathematik* 8(1), 1–13.
- Burden, R. L., J. D. Faires, and A. C. Reynolds (2001). Numerical analysis.
- Butcher, J. C. (2016). *Numerical methods for ordinary differential equations*. John Wiley & Sons.
- Calderhead, B., M. Girolami, and N. D. Lawrence (2009). Accelerating Bayesian inference over nonlinear differential equations with gaussian processes. In *Advances in neural information processing systems*, pp. 217–224.
- Campbell, D. and R. J. Steele (2012). Smooth functional tempering for nonlinear differential equation models. *Statistics and Computing* 22(2), 429–443.
- Cao, J., J. Z. Huang, and H. Wu (2012). Penalized nonlinear least squares estimation of time-varying parameters in ordinary differential equations. *Journal of computational and graphical statistics* 21(1), 42–56.
- Cao, J., L. Wang, and J. Xu (2011). Robust estimation for ordinary differential equation models. *Biometrics* 67(4), 1305–1313.

- Chen, J. and H. Wu (2008). Efficient local estimation for time-varying coefficients in deterministic dynamic models with applications to HIV-1 dynamics. *Journal of the American Statistical Association* 103(481), 369–384.
- Chopin, N. et al. (2004). Central limit theorem for sequential Monte Carlo methods and its application to Bayesian inference. *The Annals of Statistics* 32(6), 2385–2411.
- Dass, S. C., J. Lee, K. Lee, and J. Park (2017). Laplace based approximate posterior inference for differential equation models. *Statistics and Computing* 27(3), 679–698.
- De Boor, C. (1972). On calculating with b-splines. *Journal of Approximation theory* 6(1), 50–62.
- Del Moral, P. (2004). Feynman-kac formulae. In *Feynman-Kac Formulae*, pp. 47–93. Springer.
- Del Moral, P., A. Doucet, and A. Jasra (2006). Sequential Monte Carlo samplers. *Journal of the Royal Statistical Society: Series B (Statistical Methodology)* 68(3), 411–436.
- Del Moral, P., A. Doucet, and A. Jasra (2012). An adaptive sequential Monte Carlo method for approximate Bayesian computation. *Statistics and Computing* 22(5), 1009–1020.
- Dondelinger, F., D. Husmeier, S. Rogers, and M. Filippone (2013). ODE parameter inference using adaptive gradient matching with Gaussian processes. In *Artificial Intelligence and Statistics*, pp. 216–228.
- Douc, R. and O. Cappé (2005). Comparison of resampling schemes for particle filtering. In *Image and Signal Processing and Analysis, 2005. ISPA 2005. Proceedings of the 4th International Symposium on*, pp. 64–69. IEEE.
- Doucet, A., N. De Freitas, and N. Gordon (2001). An introduction to sequential Monte Carlo methods. In *Sequential Monte Carlo methods in practice*, pp. 3–14. Springer.
- Doucet, A., S. Godsill, and C. Andrieu (2000). On sequential Monte Carlo sampling methods for Bayesian filtering. *Statistics and computing* 10(3), 197–208.
- Hochbruck, M., C. Lubich, and H. Selhofer (1998). Exponential integrators for large systems of differential equations. *SIAM Journal on Scientific Computing* 19(5), 1552–1574.

- Hochbruck, M. and A. Ostermann (2010). Exponential integrators. *Acta Numerica* 19, 209–286.
- Hol, J. D., T. B. Schon, and F. Gustafsson (2006). On resampling algorithms for particle filters. In *Nonlinear Statistical Signal Processing Workshop, 2006 IEEE*, pp. 79–82. IEEE.
- Jain, M. K. (1979). *Numerical solution of differential equations*. Wiley Eastern New Delhi.
- Jameson, A., W. Schmidt, and E. Turkel (1981). Numerical solution of the Euler equations by finite volume methods using Runge Kutta time stepping schemes. In *14th fluid and plasma dynamics conference*, pp. 1259.
- Lee, K., J. Lee, and S. C. Dass (2018). Inference for differential equation models using relaxation via dynamical systems. *Computational Statistics & Data Analysis*.
- Liu, J. S. and R. Chen (1998). Sequential Monte Carlo methods for dynamic systems. *Journal of the American statistical association* 93(443), 1032–1044.
- May, R. M. (1976). Models for single populations. *Theoretical ecology*.
- Monk, N. A. (2003). Oscillatory expression of Hes1, p53, and NF- κ B driven by transcriptional time delays. *Current Biology* 13(16), 1409–1413.
- Neal, R. M. (2001). Annealed importance sampling. *Statistics and computing* 11(2), 125–139.
- Nicholson, A. J. (1954). An outline of the dynamics of animal populations. *Australian journal of Zoology* 2(1), 9–65.
- Pang, T., P. Yan, and H. H. Zhou (2017). Asymptotically efficient parameter estimation for ordinary differential equations. *Science China Mathematics* 60(11), 2263–2286.
- Poyton, A., M. S. Varziri, K. B. McAuley, P. McLellan, and J. O. Ramsay (2006). Parameter estimation in continuous-time dynamic models using principal differential analysis. *Computers & chemical engineering* 30(4), 698–708.
- Ramsay, J. O. (2004). Functional data analysis. *Encyclopedia of Statistical Sciences* 4.

- Ramsay, J. O., G. Hooker, D. Campbell, and J. Cao (2007). Parameter estimation for differential equations: a generalized smoothing approach. *Journal of the Royal Statistical Society: Series B (Statistical Methodology)* 69(5), 741–796.
- Ramsay, J. O. and B. W. Silverman (2007). *Applied functional data analysis: methods and case studies*. Springer.
- Reiss, P. T. and R. Todd Ogden (2009). Smoothing parameter selection for a class of semiparametric linear models. *Journal of the Royal Statistical Society: Series B (Statistical Methodology)* 71(2), 505–523.
- Rosenzweig, M. L. and R. H. MacArthur (1963). Graphical representation and stability conditions of predator-prey interactions. *The American Naturalist* 97(895), 209–223.
- Soetaert, K., T. Petzoldt, and R. W. Setzer (2010). Solving differential equations in R: package desolve. *Journal of Statistical Software* 33.
- Varah, J. M. (1982). A spline least squares method for numerical parameter estimation in differential equations. *SIAM Journal on Scientific and Statistical Computing* 3(1), 28–46.
- Wang, L. and J. Cao (2012). Estimating parameters in delay differential equation models. *Journal of agricultural, biological, and environmental statistics* 17(1), 68–83.
- Wang, L., S. Wang, and A. Bouchard-Côté (2019). An annealed sequential Monte Carlo method for Bayesian phylogenetics. *Systematic Biology*.
- Zhang, T., Q. Yin, B. Caffo, Y. Sun, D. Boatman-Reich, et al. (2017). Bayesian inference of high-dimensional, cluster-structured ordinary differential equation models with applications to brain connectivity studies. *The Annals of Applied Statistics* 11(2), 868–897.
- Zhou, Y., A. M. Johansen, and J. A. Aston (2016). Toward automatic model comparison: an adaptive sequential Monte Carlo approach. *Journal of Computational and Graphical Statistics* 25(3), 701–726.

APPENDIX

In this Appendix, we introduce a classical Markov chain Monte Carlo algorithm for inference of parameters in Bayesian differential equations. We follow the notation described in *Section 2*. The joint likelihood function of $\boldsymbol{\theta}$, τ , $\mathbf{x}(0)$ and $\boldsymbol{\sigma}^2$ can be written as

$$L(\boldsymbol{\theta}, \tau, \mathbf{x}(0), \boldsymbol{\sigma}^2) = \prod_{i=1}^I \prod_{j=1}^J (\sigma_i^2)^{-1/2} \exp \left\{ -\frac{(y_{ij} - x_i(t_{ij} | \boldsymbol{\theta}, \tau, \mathbf{x}(0)))^2}{2\sigma_i^2} \right\}. \quad (18)$$

To construct a Bayesian framework, we assign appropriate prior distributions for model parameters $\boldsymbol{\theta}$, τ , $\mathbf{x}(0)$ and $\boldsymbol{\sigma}^2$, denoted by $\pi_0(\boldsymbol{\theta})$, $\pi_0(\tau)$, $\pi_0(\mathbf{x}(0))$ and $\pi_0(\boldsymbol{\sigma}^2)$. The full conditional posterior distribution of σ_i^2 is Inverse-Gamma distributed. The full conditional posterior distributions of $\boldsymbol{\theta}$, τ , $\mathbf{x}(0)$ do not have analytical solutions. We conduct a random walk MH algorithm to sample new parameters. We use τ as an illustrative example. Conditional on samples at n -th iteration $\boldsymbol{\theta}^{(n)}$, $\mathbf{x}(0)^{(n)}$ and $\boldsymbol{\sigma}^{2(n)}$,

1. $\tau^* \sim N(\tau^{(n)}, \sigma_\tau^2)$.
2. Solve DEs numerically and obtain $\mathbf{x}(t_{ij} | \boldsymbol{\theta}^{(n)}, \tau^*, \mathbf{x}(0)^{(n)})$.
3. Compute the acceptance probability

$$p_{MH} = \min \left\{ 1, \frac{\gamma(\boldsymbol{\theta}^{(n)}, \tau^*, \mathbf{x}(0)^{(n)}, \boldsymbol{\sigma}^{2(n)})}{\gamma(\boldsymbol{\theta}^{(n)}, \tau^{(n)}, \mathbf{x}(0)^{(n)}, \boldsymbol{\sigma}^{2(n)})} \right\}.$$

4. Sample $u \sim U(0, 1)$, we accept $\tau^{(n+1)} = \tau^*$ if $u < p_{MH}$, otherwise $\tau^{(n+1)} = \tau^{(n)}$.